ROLE OF SULPHATE ON CORROSION INHIBITION OF ALUMINIUM ALLOY IN ACIDIC ENVIRONMENT

NORSHAMIRA BINTI MAZLAN

DISSERTATION SUBMITTED IN

PARTIAL FULFILMENT OF THE

REQUIREMENTS FOR THE DEGREE

OF MASTER OF MECHANICAL ENGINEERING

MECHANICAL ENGINEERING
UNIVERSITY OF MALAYA
KUALA LUMPUR

2022

UNIVERSITY OF MALAYA
ORIGINAL LITERARY WORK DECLARATION

Name of Candidate: Norshamira Binti Mazlan

Matric No: s2033251/1

Name of Degree: Master of Mechanical Engineering

Title of Project Paper/Research Report/Dissertation/Thesis ("this Work"): Role of Sulphate on Corrosion Inhibition of Aluminium Alloy in Acidic Environment

Field of Study: Mechanical Engineering

I do solemnly and sincerely declare that:

(1) I am the sole author/writer of this Work;
(2) This Work is original;
(3) Any use of any work in which copyright exists was done by way of fair dealing and for permitted purposes and any excerpt or extract from, or reference to or reproduction of any copyright work has been disclosed expressly and sufficiently and the title of the Work and its authorship have been acknowledged in this Work;
(4) I do not have any actual knowledge nor do I ought reasonably to know that the making of this work constitutes an infringement of any copyright work;
(5) I hereby assign all and every rights in the copyright to this Work to the University of Malaya ("UM"), who henceforth shall be owner of the copyright in this Work and that any reproduction or use in any form or by any means whatsoever is prohibited without the written consent of UM having been first had and obtained;
(6) I am fully aware that if in the course of making this Work I have infringed any copyright whether intentionally or otherwise, I may be subject to legal action or any other action as may be determined by UM.

Candidate's Signature Date: 20/8/2022

Subscribed and solemnly declared before,

Witness's Signature Date:

21 July 2022

Name:

Designation:

ROLE OF SULPHATE ON CORROSION INHIBITION OF ALUMINIUM ALLOY IN ACIDIC ENVIRONMENT

ABSTRACT

Acid accelerates the corrosion process of aluminium. In this study, sulphate is used to study the corrosion inhibition on 5052 aluminium alloy surfaces. Sodium sulphate is added into different pH of acid solution. Concentrated sodium hydroxide was used to alter the pH of concentrated hydrochloric acid to get the desired pH 2, pH 4 and pH 6. Distilled water is used to prepare pH 7 to compare the behaviour of sulphate in acid and neutral electrolytes. Potentiodynamic polarisation measurement was employed to evaluate the electrochemical characteristics of the aluminium samples. While assessing the performance of the inhibitors, the effect of inhibitor concentrations in the acidic and neutral electrolytes are also to be studied. The corrosion rates of the aluminium samples were reduced when sulphate inhibitor was added into the acidic electrolyte. It is found that the corrosion density of aluminium samples was reduced with increasing inhibitor concentration until 400 mg/L in all pH conditions and the maximum efficiency is identified at pH 6 with 67.4% . From Tafel plots, sulphate acts as anodic-dominant inhibitor in acidic environment. The corroded samples were analysed under optical microscope for surface characterisation. The morphological images study on aluminium alloy samples perceived that uniform corrosion happened on the aluminium surface with slightly pitting on certain areas.

Keywords: aluminium, sulphate, corrosion, inhibitor, acidic.

PERANAN SULFAT DALAM MERENCAT KAKISAN ALOI ALUMINIUM DI DALAM PERSEKITARAN BERASID

ABSTRAK

Asid mempercepatkan proses kakisan aluminium. Dalam kajian ini, sulfat digunakan untuk mengkaji rencatan kakisan pada 5052 permukaan aloi aluminium. Natrium sulfat ditambah ke dalam pH larutan asid yang berbeza. Natrium hidroksida pekat digunakan untuk mengubah pH asid hidroklorik pekat untuk mendapatkan pH 2, pH 4 dan pH 6. Air suling digunakan untuk menyediakan pH 7 untuk membanding sifat sulfat di dalam elektrolit berasid dan neutral. Polarisasi potensiodinamik digunakan untuk menilai ciri elektrokimia sampel aluminium. Semasa menilai prestasi perencat, kesan kepekatan perencat dalam elektrolit berasid dan neutral juga perlu dikaji. Kadar kakisan sampel aluminium telah dikurangkan apabila perencat kakisan sulfat ditambah ke dalam elektrolit berasid. Didapati bahawa ketumpatan kakisan sampel aluminium telah dikurangkan dengan peningkatan kepekatan perencat sehingga 400 mg/L dalam semua keadaan pH dan kecekapan maksimum dikenal pasti pada pH 6 dengan 67.4% . Plot Tafel menunjukkan sulfat bertindak sebagai perencat dominan anodik dalam persekitaran berasid. Sampel yang berkarat dianalisis di bawah mikroskop optik untuk pencirian permukaan. Kajian imej morfologi terhadap sampel aloi aluminium mendapati bahawa kakisan seragam berlaku pada permukaan aluminium dengan sedikit pitting pada kawasan tertentu.

Kata kunci: aluminium, sulfat, kakisan, perencat, berasid.

ACKNOWLEDGEMENTS

I would like to thank my family, supervisor, and lab staffs that had helped me throughout these semesters to finally finish my dissertation report. The research study of this paper is out of my main knowledge as a mechanical engineering student, however I managed to complete this research study with lots of motivation and support physically and verbally from these people. Thank you for examiners that provided feedback for improvement. It is honoured to be able complete my master's degree in University of Malaya, despite being the best university in Malaysia.

TABLE OF CONTENTS

LIST OF FIGURES

LIST OF TABLES

LIST OF SYMBOLS AND ABBREVIATIONS

Al : Aluminium

$Al(OH)_3$: Aluminium hydroxide

Al_2O_3 : Aluminium oxide

Al^{3+} : Aluminium ion

Cl^- : Chloride ion

CS : Chondroitin sulphate

DMImCl : Imidazolium ionic liquid

E_{corr} : Corrosion potential density

EDX : Energy dispersive X-ray

H^+ : Hydrogen ion

HCl : Hydrochloric acid

I_A : Corrosion current density in anode

I_C : Corrosion current density in cathode

I_{corr} : Corrosion current density

I_I : Corrosion current density in inhibited solution

I_o : Corrosion current density in uninhibited solution

mmpy : Millimetre per year

N : Nitrogen

Na_2SO_4 : Sodium sulphate

NH_4Cl : Ammonium chloride

NO_x : Nitrogen oxide

OCP : Open circuit potential

P : Phosphorus

S : Sulphur

SDS	:	Sodium dodecyl sulphate
SEM	:	Surface Electrons Microscope
SO_2	:	Sulphur dioxide
SO_4^{2-}	:	Sulphate ion
T	:	Immersion period
βa	:	Anodic slope
β_c	:	Cathodic slope
ρ	:	Density
ΔW	:	Weight loss

LIST OF APPENDICES

CHAPTER 1: INTRODUCTION

1.1 Background

Aluminium is prevalent in various manufacturing industries, especially in transportation, construction, and consumer goods. This is due to its attractive qualities, such as being strong, lightweight, durable, and resistant to corrosion. Aluminium is usually alloyed to increase its strength and applications. The Aluminium Association (AA Inc.) has created numerous aluminium alloys based on their alloying constituents, each with a four-digit designation (Schweitzer, 2010). 5052 aluminium alloy will be the focus of this research, which belongs to the 5xxx series of aluminium alloys or those containing magnesium as their primary alloying alloy. The 5052 aluminium alloy is essential to its enhanced resistance to corrosive environments. In the presence of air/water, all aluminium alloys generates an oxide layer, which shields the chemically active aluminium from interacting further with the surrounding environments. Corrosion resistance varies according to temperature, airborne pollutants, and the immediate working environment; nonetheless, 5052 aluminium alloy performs remarkably well under ambient conditions. There are many applications for 5052 aluminium alloy, but some significant ones include marine equipment, such as ships, aircraft welding parts, and parts of oil pipes in oil and gas (O&G) industries. However, with prolonged immersion or exposure to aggressive pH environments and solution containing chloride ions, the protective oxide layer of aluminium will be easily destroyed, which reduces the corrosion-resistant ability. Aluminium alloys can encounter aggressive media in many requirements such as in acid rain, mud and in solutions used for cleaning which contains chloride ions. Chloride ions also present in pickling, chemical and electrochemical etching of metals and alloys (Pyun & Lee, 2001; Trompette & Lahitte, 2021; Zhang et al., 2021). Corrosion leads to fatigue and catastrophic failure of metal. Thus, this unwanted property needs to be addressed accordingly. Corrosion inhibitors are typically used to reduce corrosion in acidic media, especially in commercial cleaning processes, oil and gas production, pulp and paper industry, and corroded metal artefacts, because they are effective and cheap. There are many classifications of corrosion inhibitors, but the most popular inhibitors to prevent corrosion in an acidic environment are organic inhibitors such as nitrogen-, sulphur,- and oxygen-containing compounds and pi-electrons compounds (Metikoš-Huković et al., 1994; Nathiya et al., 2017; Nwanonenyi et al., 2019). It was claimed by Pyun et al. (1999) that the addition of $SO^{2-}{}_4$ ions decreased the anodic dissolution of aluminium in alkaline solution and does not cause pitting in all pH ranges. The statement is backed up by the found made by Beccaria and Poggi (1987) where the addition of 0.01 to 0.1 M SO_4^{2-} blocked the corrosion of aluminium in slightly alkaline electrolytes through adsorption mechanism. However, the electrochemical noise study reported by Na and Pyun (2007), it was described that the presence of SO_4^{2-} ion escalates the corrosion of aluminium in aqueous alkaline solution. The most recent literature by Li and Church (2018) on the analysis of SO_4^{2-} ion, it is believed that the chemical adsorption of SO_4^{2-} ion changes the composition of the passive oxide film on the surface of aluminium. To the best knowledge, there is limited to no literature describing the effects of SO_4^{2-} ion on 5052 aluminium alloy in aqueous acidic environments. In this study, sodium sulphate is used to study the effect of sulphate on corrosion inhibition of aluminium alloy in the aqueous acidic media. The 5052 aluminium alloy is subjected to an immersion test in different acidic environments, with pH ranging from 2 to 7, varying the sodium sulphate inhibitor concentration. The corrosion evaluation consists of measuring the weight loss of the metal, getting a Tafel plot from the potentiodynamic polarization technique and surface study using optical microscopy.

1.2 Objectives

The objectives of this research project are:

1. To study the influence of sulphate ions concentration on corrosion of aluminium alloy.
2. To understand sulphate ions corrosion inhibition on aluminium alloy.
3. To characterise the corrosion morphology of aluminium alloy in acidic environment.

1.3 Research problem

Acidic corrosion is a gradual destruction of and wearing away of a material due to acidic compounds present in the environment. In boilers and furnaces, this corrosion is caused by the presence of corrosive ions such as chloride in chemical cleaning. The presence of other anion species such as sulphate ions could change the corrosion morphology of aluminium alloy by sharing its electron to metal surface instead of chloride ions. Therefore, it is crucial to assess the capability of sulphate ions to subdue the corrosion of metal in an acidic environment using electrochemical reaction and potentiostat method.

CHAPTER 2: LITERATURE REVIEW

2.1 Aluminium and Aluminium Alloys

Aluminium and its alloy are globally used in manufacturing industries, including automobiles, aircraft, household appliances, and electronic devices. Unalloyed aluminium offers unique qualities that limit its usage only in a few engineering applications. The properties of aluminium, such as mechanical properties, formability, or weldability, can be increased or modified by adding small quantities of other metals to base aluminium, be it copper, magnesium, iron, or manganese, to create aluminium alloys. Aluminium alloys are available as castings or wrought-rolled semi-products (Hussey & Wilson, 1998). A four-digit numbering system is used to classify wrought aluminium and aluminium alloys depending on their primary alloying elements, as illustrated in Table 2.1 (Ross, 1992).

Table 2.1: Series designation of wrought aluminium and its alloy.

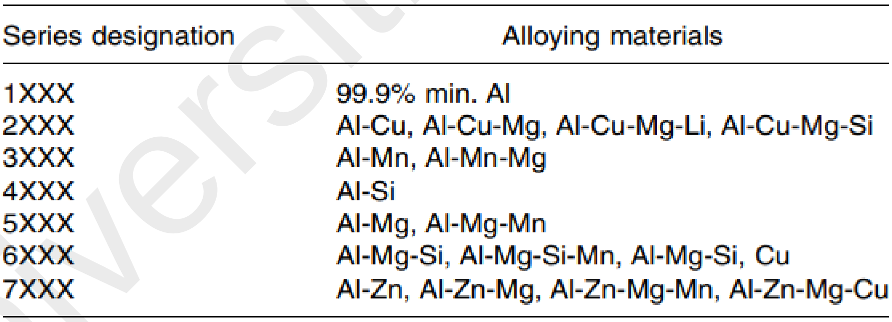

Series designation	Alloying materials
1XXX	99.9% min. Al
2XXX	Al-Cu, Al-Cu-Mg, Al-Cu-Mg-Li, Al-Cu-Mg-Si
3XXX	Al-Mn, Al-Mn-Mg
4XXX	Al-Si
5XXX	Al-Mg, Al-Mg-Mn
6XXX	Al-Mg-Si, Al-Mg-Si-Mn, Al-Mg-Si, Cu
7XXX	Al-Zn, Al-Zn-Mg, Al-Zn-Mg-Mn, Al-Zn-Mg-Cu

The American National Standards Institute (ANSI) standard H35.1 has specified these alloy numbers and their related tempers. The second digit in the 1XXX group indicates the purity of the aluminium used to produce the respective grade. For example, zero in the 10XX grade denoted that aluminium is fundamentally pure, whilst 1 to 9 indicate a particular control of one or more specific impurity elements. The second digit in the 2XXX until the 7XXX alloy group indicates an alloy alteration. The major alloying element is shown in Table 2.2 below (Ross, 1992).

Table 2.2: Major alloying ingredient of wrought aluminium and its alloy.

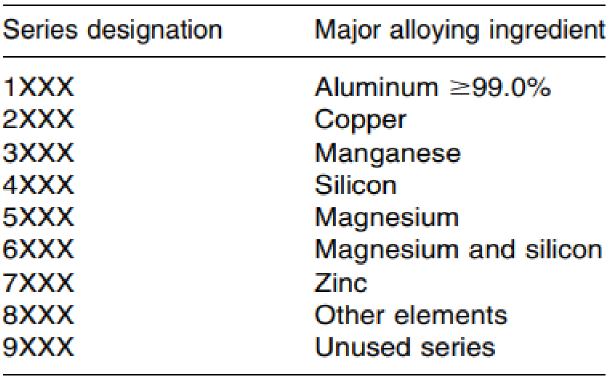

Series designation	Major alloying ingredient
1XXX	Aluminum ≥99.0%
2XXX	Copper
3XXX	Manganese
4XXX	Silicon
5XXX	Magnesium
6XXX	Magnesium and silicon
7XXX	Zinc
8XXX	Other elements
9XXX	Unused series

2.1.1 Physical metallurgy

The most common wrought aluminium alloys are 1000, 2000, 3000, 5000, 6000, 7000, and 8000 series. The 1000 series is used to manufacture electric condensers, lightning devices, and high-end packaging because it compromises good resistance to mechanical, plastic deformation capability, and aesthetic appearance. The 2000 series has superior mechanical strength, low crack propagation, and good heat resistance, mainly used in aircraft construction and armament. The main applications for the 3000 series are in the building sector, heat exchanger tubing, circle for kitchen utensils, fabrication, sheet metal work, etc. Alloy 5000 series is used in many applications in commercial vehicle bodies and road signs and can be used in foodstuffs such as beverage cans and especially in maritime environments. The 6000 series is generally used in diverse technology fields such as mechanics applications, railcars, and pipelines, while the 7000 series is often used in mechanical, aviation and recreational equipment. The 8000 series has a fine grain structure which boosts its utilisation as fins for heat exchangers, thin foil, e.tc (Hussey & Wilson, 1998).

2.1.2 Mechanical properties

Aluminium has the benefits of being lightweight with a density of 2.7 g/m3 compared to iron of 7.83 g/m^3, resistance to corrosion, simplicity of production, and appearance as a structural metal. Its alloys have approximately three times the strength of structural steel in terms of strength-to-density ratio and are reasonably equivalent to the steel used in gears, shafts, and axles. Aluminium alloys have high resistance to corrosion in various media such as waters, atmospheres, chemicals, and other materials. Their salts are harmless, enabling them to be used in canned beverages, foods, and medications. They are white or colourless, allowing them to be used with chemicals and other materials without staining, and are eco-sustainable. High electrical conductivity, thermal conductivity, reflectivity, and non-magnetic are all attractive traits of aluminium and its alloy (Hussey & Wilson, 1998). The application of aluminium for the oil and gas industry has become essential in this industry, with the main reason being extreme importance of structure weight in deep offshore field exploration and development.

2.1.3 Passive film on aluminium surface

Aluminium is known as a passive metal due to the presence of a thin, excellent adherent film of oxide on its surface. Aluminium's surface film immediately appears and proliferates when a new aluminium surface is exposed to the air or water(Hassan et al., 2018). The passive film on the aluminium surface made it resists corrosion in various environments. The stable, protective film thickness formed in the air and water at ambient temperature is approximately 5 nm thick (Zhao et al., 2017). When the environment’s temperature increases in the presence of water and oxygen, the oxide film begins to thicken. According to Pourbaix diagram in Figure 2.3.1.1, the thermodynamic circumstances under which this film develops in aqueous solutions, aluminium is only passive in the pH range of 4 to 9 (Pedeferri, 2018a).

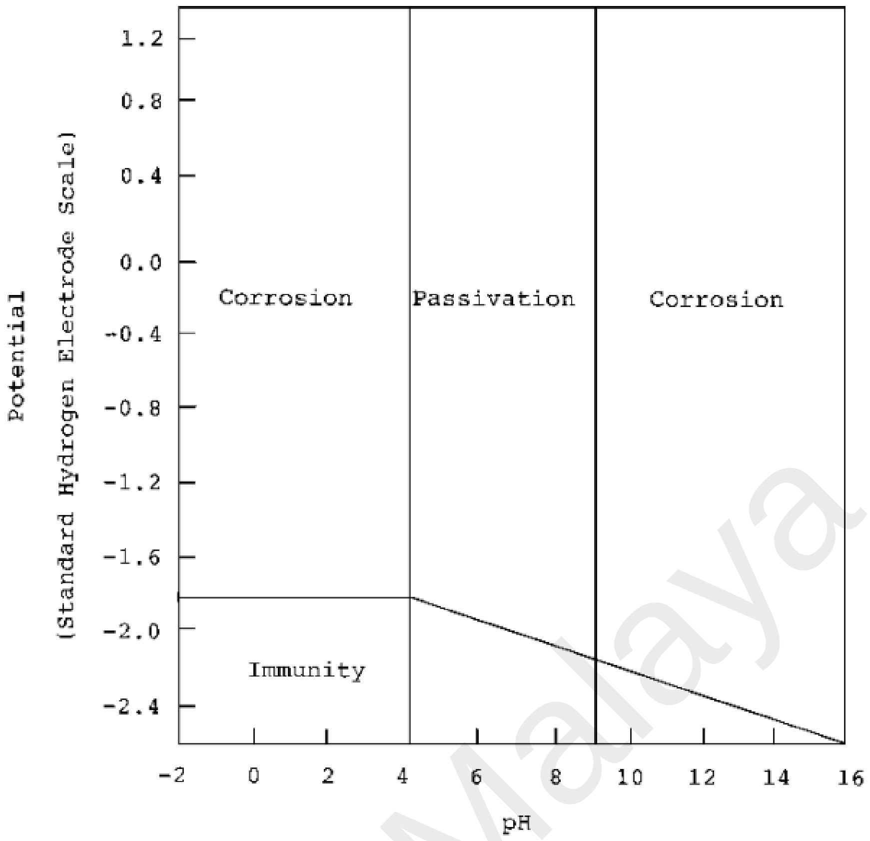

Figure 2.1: Pourbaix diagram of aluminium at ambient temperature.

As shown in figure 2.1, aluminium corrodes in both acidic and alkaline environments. Al^{3+} ions are formed at a lower pH, and Al_2O_3 are produced at a higher pH. There are exceptions when the protective oxide film is insoluble in acidic or alkaline solution, and the oxidising nature of the solution keeps it in place. It is when the electrolyte is acetic acid, ammonium hydroxide with a concentration of more than 30 % by weight, the nitric concentration of more than 80 % by weight, or sulphuric acid with a concentration of 98 – 100 % by weight. Aluminium also has the tendency to corrode due to flaws in its protective oxide layer (Pedeferri, 2018b; Ross, 1992).

2.1.4 Passivity in various pH environments

The dissolution rate of aluminium is higher in strong acidic and strong alkaline solutions shown in figure 2.2 below:

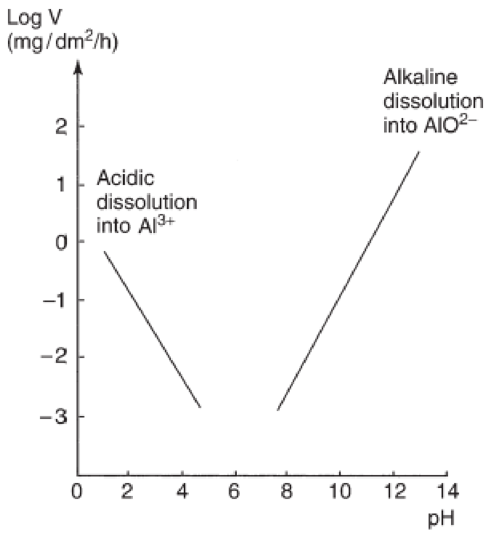

Figure 2.2: Rate of dissolution of aluminium on different pH.

The aluminium rate of dissolution is not solely dependent on the pH value of the medium, but the nature of the acid or base also plays a significant role. In industries, acidic solutions are often employed for surface cleaning, which is compulsory for all metals, including the metal with expensive coatings (Raviprabha & Ramesh, 2019). In the presence of an acidic medium such as hydrochloric acid (HCl), the protective oxide layer gets broken by chloride (Cl^-) ions. L'Haridon-Quaireau et al. (2020) studied the effect of pH on corrosion behaviour of aluminium alloy mentioned that the film on the aluminium surface consist of two layers and one of it is aluminium hydroxide phase. Corrosion behaviour of aluminium depend on the pH of electrolyte. The author mentioned that high pH medium has higher corrosion rate compared to low pH because higher pH encourage aluminium to absorb more aluminium hydroxide. High solubility of aluminium hydroxide decreases its ability as a protective film, thus increase aluminium corrosion. The nature of acids and bases also affect the dissolution of aluminium. For example, hydrochloric acid is much more aggressive towards aluminium than sulphuric acid for the acidic medium (Ćurković et al., 2008). Figure 2.3 shows the average penetration of aluminium in different acids and bases.

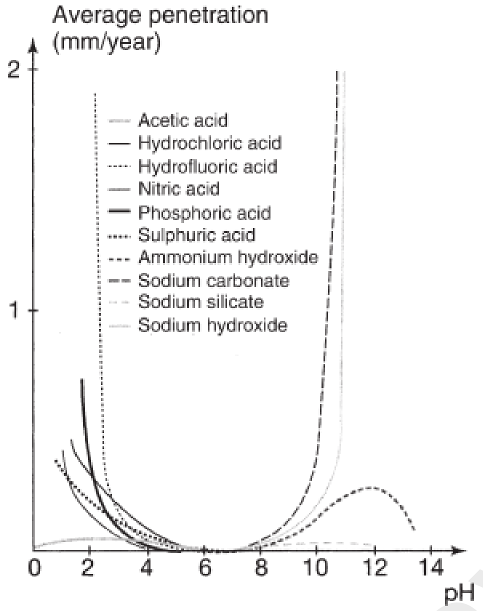

Figure 2.3: The penetration of aluminium depends on the nature of acids and bases.

Aluminium is susceptible to pitting corrosion in a neutral aqueous environment which makes it belongs to passive metals group. This is acknowledged by Peng et al. (2022) after exposing aluminium in the marine atmosphere for five months. The author found that oxygen can easily approach the aluminium surface and caused major pitting corrosion by cathodic reactions.

2.2 Corrosion

Corrosion is a gradual, persistent, or quick degradation of metal properties such as appearance, exterior element, or mechanical performances because of the surrounding environment, which includes the atmosphere, electrolyte, chemicals, and other materials. This corrosion process is a significant impediment to the lifetimes since it frequently resulting in deterioration and failure of the metal in its applicability. Enormous expenditures for maintenance, replacements, and technical services are necessary to address these drawbacks. These undesirable flaws that related to corrosion of metals have resulted in the emergence of worldwide industries dedicated to suppress and reducing the initiation of corrosion or to minimise the negative consequences it has on its associated application ("dissimilar (metal) corrosion," 2014). Metal corrosion reaction in electrolyte environment is the summation of two electrochemical reactions which are an anodic process (oxidation of metal) and a cathodic process (reduction reaction, usually oxygen reduction and hydrogen evolution).

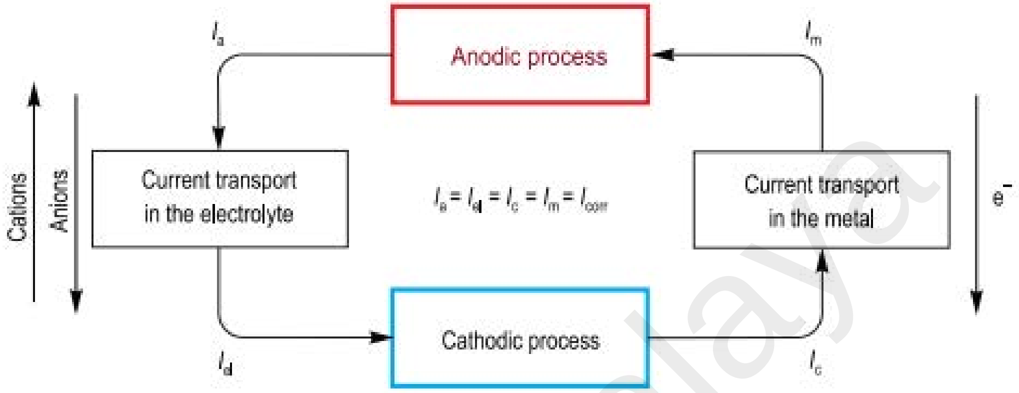

Figure 2.4: Electrochemical mechanism of corrosion.

(Pedeferri, 2018b) summarised the corrosion process into four stages in series as shown in Figure 2.4. These four stages occur at equal rate because of the electroneutrality law which the cathodic reaction consumes the electrons produced by the anodic reaction in a timely manner:

$$\mathbf{I_a = I_c = I_m = I_{el} = I_{corr}}$$

Where I_{corr} is the corrosion rate, measured in electrochemical unit. Corrosion changes the physical and mechanical properties of a metal. The effects are manifested in two types which are uniform and localised corrosion (crevice, pitting etc.). These attacks cause the reduction in the thickness and weight of the metal. Typically, aluminium suffers from corrosion in average of 0.001 mils/y, but it can change depend on the conditions of the environment. For example, in the industrial environment, the corrosion rates is averaged at 0.03–0.11 mils/y and can reach as high as 0.52 mils/y if it is exposed in a polluted air (Ahmad, 2006).

2.2.1 The electrochemical of aluminium corrosion

Aluminium corrosion is generated by the electrochemical interaction of a metal or alloy and an electrolyte associated with the atomic structure of matters. The matter comprises electrically charged elementary particles, such as ions and electrons, and electrically neutral particles. Atoms in metals exist in an electrical environment comprised of free atoms that move freely throughout the metal. The positive, negative, and uncharged species can be found in the aqueous. The transfer of electric charges at the metal-water interface causes electrochemical reactions. The oxidation of aluminium in water:

$$\mathrm{Al} \rightarrow \mathrm{Al}^{3+} + 3\mathrm{e}^{-}$$

(1)

It causes a flux of electrons within the aluminium or an anodic current, I_a flows in the direction metal → solution, which takes place in the anode.

In the oxidation pH state, aluminium metal loses three electrons; therefore, the oxidation state goes to 0. This reaction is balanced by the reduction process, which captures emitted electrons. Reduction of H^+ protons in water:

$$3\mathrm{H}^{+} + 3\mathrm{e}^{-} \rightarrow \frac{3}{2}\mathrm{H}_2$$

(2)

It causes a flux of electrons from the metal, or a cathodic current I_c flows in the direction of the solution→ metal that takes place in the cathode.

Reduction of oxygen in acidic (Equation 3) and alkaline/neutral medium (Equation 4);

$$\mathrm{O_2 + 4H^+ + 4e^- \rightarrow 2H_2O}$$

(3)

$$\mathrm{O_2 + 2H_2O + 4e^- \rightarrow 4OH^-}$$

(4)

Generally, the addition of two electrochemical processes, oxidation, and reduction of aluminium in an electrolyte:

$$\mathrm{Al \rightarrow Al^{3+} + 3e^-}$$

(5)

$$\mathrm{3H^+ + 3e^- \rightarrow \frac{3}{2}H_2}$$

(6)

$$\mathrm{Al + 3H^+ \rightarrow Al^{3+} + \frac{3}{2}H_2}$$

(7)

Or rearrange equation 7 becomes

$$\mathrm{Al + 3H_2O \rightarrow Al(OH)_3 + \frac{3}{2}H_2}$$

(8)

The production of aluminium hydroxide, $Al(OH)_3$ is the result of aluminium corrosion, not soluble in water and crystallised as white gel, which can also be observed as thick white flakes in corrosion pits.

The electron and current fluxed are in balance when metal is electrically isolated,

$$\sum I_a = \sum I_k$$

except when the electrodes are connected to a generator.

All electrochemical processes in a particular system result in electrical currents determined by the potential differences between the metal and electrolyte. The kinetic electrochemical reactions of anodic and cathodic are depicted by the correlation between the potential E_{corr} and the current density I shown in Figure 2.5:

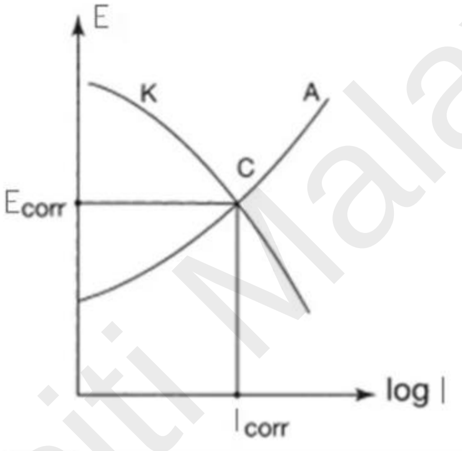

Figure 2.5: Graph of current density against potential.

For natural corrosion, the system produced by the metal and the electrolyte comprises an open electrical circuit without an external source of electric current. No current movement from the metal to the solution or conversely. The anodic and cathodic currents, flow in opposite ways, must be equal (at point C). the intersection of the two polarization curves establishes the corrosion potential E_{corr} and the intensity of corrosion I_{corr}. Faraday's Law states that:

$$m = \frac{1}{96\ 500}\frac{A}{n}It \qquad (9)$$

Where m is the metal mass, A is the atomic mass of aluminium, n is the, I is the intensity (A), I_{corr}, and t is the time (s). The corrosion rate can be calculated from the mass loss using the intensity and exposure period. It is not applicable for non-uniform corrosion on metal.

2.2.2 Thermodynamic environments

Thermodynamic environment for a voluntary corrosion mechanism is $\Delta G < 0$, which transforms into the following potential:

$$\Delta E > 0;\ E_C > E_A$$

where $\Delta E = E_C - E_A, E_C$ and $E_A$is the potential of the cathodic and anodic processes respectively. The corrosion process is spontaneous if cathodic potential is higher than anodic potential (Pedeferri, 2018b).

2.2.3 Factors That Influence Corrosion

There are many factors that affect the nature and extent of corrosion process that can be classified as primary and secondary.

2.2.3.1 Primary factors

Nature of metal: Metals with lower electrochemical potential is more susceptible to corrode while metals compared to higher electrochemical potential metals. Some of the reactive metals that easily corrode are sodium (Na), potassium (K), magnesium (Mg) and zinc (Zn). The noble metals such as ruthenium (Ru), palladium (Pd), platinum (Pt) and silver (Ag) are stable and do not corrode easily especially in ambient atmosphere.

Surface condition of metal: Metals with rough surface suffer corrosion compared to smooth surface because the air can be trapped easily on the irregular texture of metal.

Corrosion product: The insoluble, stable, and uniform corrosion product acts like a barrier or protective film of the metal surface and prevent further corrosion. Corrosion continues if the corrosion product is soluble, unstable, and non-uniform corrosion.

Hydrogen overpotential: Elevated hydrogen overvoltage slows down or halt the cathodic reaction of metals. As cathodic reaction decreases, corrosion rate decreases.

2.2.3.2 Secondary factors

pH of electrolytes: The presence of oxygen is crucial for corrosion to take place on metal. pH low than 3 have higher corrosion rate because oxygen undergoes continuous hydrogen evolution. For pH greater than 10 favours the formation of metal hydrous oxide which acts as protective film that minimise corrosion process.

Temperature: As temperature increased, the corrosion protective film becomes more refine and compact, indicating better corrosion resistant on metal surface. It also increases the conductance of aqueous media, resulting more faster exchange of electrons at electrode surfaces.

Impurities and humidity: Metals in humid atmosphere is prone to corrosion compared to in dry atmosphere. Humidity creates a conducting medium for transfer of electrons and dissolution of impurities that promote corrosion process. The presence of impurities such as HCl, SO_2, and NO_x in the atmosphere can be the result of coal burning and many manufacturing activities.

Exposed area: If the cathodic area is larger than anodic area, the rate of corrosion will be faster because the electrons released by the anode are consumed quickly at the cathode.

2.2.4 Type of corrosion

Corrosion depends on the environment surrounding the material, chemical reaction, or metal treatments etc. These are the main types of corrosion:

2.2.4.1 Uniform Corrosion

Uniform or general corrosion occurs when corrosion happens evenly on the surface of an aluminium. It is the result of continual movement of anode and cathode areas in contact with the electrolyte which appears as uniform corrosive assault on the surface. The most common case of aluminium that suffer from widespread corrosion when it is exposed in low or high pH solution. This type of corrosion occurs more frequently with aluminium than other metals in strong acid or strong base solution, where the protective oxide barrier is highly soluble. The formation of protective barrier is weaker than its dissolution rate, and both rates might fluctuate with time (Pedeferri, 2018b) .

In acidic environment, passive metal such as aluminium can meet one of these conditions when there is no depassivation:

Absence of chloride. The exchange current density of hydrogen evolution is higher than passive current density of metals, so the free-corrosion and hydrogen evolution potentials are equal and the driving potential for hydrogen evolution is zero.

Presence of chloride. The exchange current density of hydrogen evolution is less than passive current density of metals, leading to a free-corrosion potential lesser than the equilibrium of potential hydrogen evolution.

2.2.4.2 Pitting Corrosion

The appearance of asymmetrical shaped voids on metal surface due to the random attacks on the particular parts of metal surface is the localised type of corrosion. The corrosion depth is affected by the media, metal condition and service circumstances. In neutral pH, aluminium is susceptible to pitting corrosion resulting from the localised rupture of oxide film. Polarization studies show that pit is passivated when it stops growing. These passivated pits are not reinitiated again when the metal is polarised; pitting begins on new spots. In cathodic locations, the oxygen gradually decreases. The presence of halide ions, mainly chloride, frequently develops pitting corrosion. Aluminium is oxidised when the film is cracked and forms $AlCl^{4-}$. Figure 2.6 shows the mechanism of pitting corrosion on the surface of the aluminium.

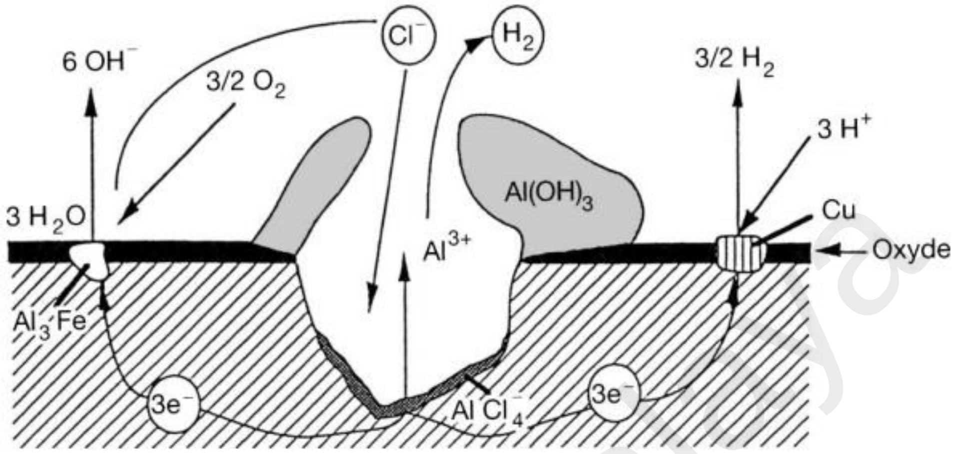

Figure 2.6: Pitting corrosion on the aluminium surface.

Oxidation at the bottom of the pit:

$$2Al \rightarrow 2Al^{3+} + 3e^-$$

(10)

Reduction outside the cavity:

$$6H^+ + 6e^- \rightarrow 3H_2$$

(11)

The overall electrochemical reaction of pitting corrosion on aluminium:

$$2Al + 3H_2O + \frac{3}{2}O_2 \rightarrow 2Al(OH)_3$$

(12)

$Al(OH)_3$ appears as a residue. The reduction of H^+ ions pushes $Al(OH)_3$ to the pit's opening and produces a deposit of white pustules. In the recent study by Peng et al. (2022), when aluminium is exposed in an almost neutral pH electrolyte, the initial oxide film is gradually destroyed over time and the corrosion products are distributed on the metal surface randomly. Cl^- ions that exist in atmospheric environment due to several reason (acid rain, polluted air, etc.) also participated in the corrosion reaction which favours pitting to happen on the metal surface. Ju et al. (2021) investigated the corrosion on the surface of aluminium and AA2024 by simultaneous electrochemical measurements and imaging found that pitting increases when the concentration of Cl^- increases in the electrolyte. Cl^- ions penetrate and adsorb strongly on aluminium surface which cause the rupture of the protection of the passive film. The breakdown of the passive film exposes the aluminium surface and made the H^+ into contact, thus further corrosion. L'Haridon-Quaireau et al. (2020) explained that the in neural and base pH environments, aluminium alloy is prone to pitting while in acid pH, aluminium alloy undergoes uniform corrosion. However, pitting corrosion on aluminium alloy surface is less impactful compared to uniform corrosion. Aluminium corrodes when the initial protective layer is ruptured, and then form pits. The depth of pits is constant over time and the thickness of passive film appeared on metal surface which is associated to uniform corrosion. The formation of aluminium hydroxide gradually passives pits and stops their growth. In contradict to L'Haridon-Quaireau et al.'s finding, Liang et al. (2018) pointed out that intensive pitting and extreme corrosion occurred on aluminium alloy after two years of exposure. Deep and shallow pits can be observed on aluminium surface under the scanning electron microscope (SEM). This shows that the severity of localised and pitting corrosion on aluminium depends on the immersion environment, exposure period and oxygen availability.

2.2.4.3 Crevice Corrosion

A localised type of corrosion occurs when metal-to-metal or metal-to-nonmetal contact where the local differences in oxygen from the small amounts of liquid are collected and become stagnant on deposits on the metal surface, gaskets or in the narrow opening between two fastened parts (Maddela & Carlson, 2019). Crevice corrosion can take place on any metal and in any corrosive media. The corrosion inside and outside the crevice undergoes the same process in a corrosive environment. After the attack starts within the crevice, it progresses very fast and is more intense in the presence of chloride ions. Cations accumulated inside the crevice attract the anions from the environment and destroy the passive film (Farfan-Cabrera et al., 2021). Maddela and Carlson (2019) investigated the corrosion behaviour of aluminium/galvanized steel resistance spot welding (RSW) and self-piercing riveting (SPR) joint in 3 % NaCl solution. The authors discussed that crevice corrosion is severe in Al/steel joints in saline and neutral pH environment compared to lower or higher pH environment.

2.2.4.4 Intergranular Corrosion

Small crystals or grains exist in the composition of metals and alloys, and their surfaces connect with each other forming grain boundaries. The penetration of other metal objects along the grain boundaries results in destruction of metals or weakening of the grains. This type of corrosion occurs when metals are heated such as welding, stress heating or laser shock peening etc. (Kaufman et al., 2022).

2.2.4.5 Galvanic Corrosion

When two dissimilar metals are electrically connected and immersed in an electrolyte, the more reactive metal acts as an anode whereas the less reactive metal acts as cathode. The ions/particles flow freely in the presence of electrolyte, resulting in fast eroding of the anode metal while the cathode metal stays uncorroded. This type of corrosion occurs in almost every joint used in industrial and structural applications (Kamble et al., 2022; Pan et al., 2021).

2.2.5 Corrosion Inhibitor

Corrosion inhibitors are widely used in a variety of industries to suppress or minimise the corrosion process of metals. It is effective in small concentrations when it is added in corrosion system at optimal conditions to reduce the metal corrosion process. These corrosion inhibitors slow the rate of the anodic oxidation, cathodic reduction or both reactions by chemical or physical adsorption on the surface of the metal. Inhibitors can be organic or inorganic and they are frequently proprietary, difficult to understand their interaction with electrochemical processes (Monticelli, 2018).

2.2.5.1 Classification of Inhibitors

There are several ways to categorise inhibitors, and several of them overlap, but the most common approach is to divide them according to their function in retarding the cathodic, anodic or both reactions of the corrosion mechanism. They either produce a shift in corrosion potential of the inhibited metal toward the cathodic or anodic directions, or they keep the metal corrosion potential nearly unchanged. The inhibition of cathodic and anodic corrosion processes are the change in the activation energy due to the oxidation or reduction reactions and/or the reducing of active surface area of a metal. A mixture of cathodic and anodic corrosion inhibitors may increase protection while also lowering inhibitor concentrations (Cui et al., 2021). The inhibitors interact with the metal-electrolyte contact by generating a film, which is either passive-, precipitate-, or adsorbed-typed film.

(a) ***Passive Inhibitors***

Passive inhibitors force the metallic substrate into passivation. The ions that act as passivators must have the thermodynamic oxidising capacity and that is readily reduced.

The least expensive inhibitor to use in water systems and internal combustion engines is chromatics. The usage of chromates has recently been subjected to new environmental laws because of toxicity concerns, and cause rashes for prolonged contact with the skin. Nitrates are used to inhibit corrosion in the machining of materials and act as an antifreeze-type cooling water system. Their inhibition works only in environments above pH 6, and tends to decompose, forming volatile nitric acid and nitrogen peroxide in an acidic environment. When the concentration of passive inhibitors fall below minimum limits, they expedite the corrosion and cause pitting. The microstructure and composition of the corrosion layer are both affected by the corrosion inhibitor (Li et al., 2021).

(b) ***Precipitation Inhibitors (Cathodic Inhibitors)***

This type of inhibitors forms precipitates on the metal of the surface which acts as a protective film. It reduces the corrosion rate of metal by interfering the cathodic processes. Calcium and magnesium carbonates are usually found in natural waters creating a protective barrier on the metal surface by precipitating with the adjustment of pH. There is a category of cathodic inhibition called hydrogen evolution poisons which retard the overall rate of the cathodic reaction of hydrogen evolution by interfering with the formation of hydrogen gas. The compounds that act as hydrogen evolution poisons are arsenic, antimony, and bismuth. These inhibitors are effective in strong acids due to the hydrogen evolution rate controlling the corrosion process (Qian et al., 2022).

(c) ***Organic Inhibitors***

A crucial factor of efficiently an organic molecules functions to inhibit corrosion is the strength of the inhibitor-substrate bonding, with stronger bond correlating with better inhibition. Majority of the organic compounds used for corrosion inhibitor have heteroatoms, unsaturated bond/aromatic rings that can donate lone pairs of electrons such as sulphur (S), phosphorus (P), and nitrogen (N). The unshared electron pairs exist as cationic/protonated forms in electrolytic media. The counterions of electrolytes interact with the positively charged metallic surface, cause the surface to become negatively charge. Two opposite charged ions attract each other by electrostatic force. There is also covalent bonding between an organic inhibitor and metallic surface, which the electron-rich group attached firmly to the substrate. The overall inhibitor composition and functional group influence the electron density and polarizability, which affect bond strength. The polar group in the molecular structure adheres itself to the metal (Monticelli, 2018). During the metal-inhibitor interactions, the extra electrons of heteroatoms and pi-electrons that are non-bonded get donated into the d-orbital of the metal surfaces that results in the establishment of coordinate bonding between them (Jessima et al., 2020). Other organic compounds such as amines, imines, thiourea, mercaptans, guanidine and aldehydes create a protective film on the metal surface that obstruct both anodic and cathodic processes. Adsorbed inhibitor molecules reduce corrosion rate by limiting oxygen diffusion and water excess to metal surface. Raviprabha and Ramesh (2019) studied the effect of 5-(3-pryridyl)-4H-1,2,4-triazole-3-thiol as corrosion inhibitor for aluminium alloy in 1 M hydrochloric acid reported that a clear adsorption process by N and S atoms was seen on aluminium surface which obey Langmuir and Flory-Huggins's adsorption isotherms. A protective film formed on the aluminium surface prevents further corrosion. Thermodynamic parameters analysis by the author found that the inhibitor acts as mixed-type inhibitor. Prakashaiah et al. (2018) found that the charged transfer from N and S atoms in organic inhibitor to the aluminium surface film effects the corrosion process. The inhibitor is adsorbed and formed oxide layer contributing to addition protective barrier known as double layer. Generally, the organic compounds with benzene rings such are the most effective inhibiting corrosion because its molecular structure made up of double bonds and rich with electrons. Thus, the shape and size of the molecular structure of the organic compound determine the adsorption onto metal surfaces, which lead to corrosion inhibition efficiency (Abdallah et al., 2019; Chen et al., 2021). As the chain length of the primary amines increases, the diffusive barrier also increases and inhibit corrosion (Jessima et al., 2020).

2.2.5.2 Physical and Chemical Adsorption

Adsorption is the key factor for corrosion inhibiting process, mainly for organic inhibitors, which their overall inhibition mechanism is by preliminary adsorption. Physical adsorption or physisorption can be due to electrostatic between inhibitor molecules (ions or dipoles) and the electrically charge metals surface, while chemical adsorption is the formation of a bond with electrons transfer from the inhibitor to the metal (Monticelli, 2018). In corrosion inhibition studies, Tafel polarization measurements and Langmuir adsorption isotherm model is often carried out to investigate the adsorption process and the appearance of protective film on metallic surface (Ishwara Bhat & Alva, 2011; Nnaji et al., 2019; Sabet Bokati & Dehghanian, 2018). The Langmuir isotherm represents an increase in surface occupancy as a function of pressure until the whole surface area is covered with a single layer of molecules and no further adsorption can take place (Ye et al., 2021). In a neutral pH environment, the 1-H-benzotriazole inhibitor was able to prevent corrosion on aluminium, mild steel, and copper through the adsorption process on metal surfaces, which physisorption is more dominant than chemisorption. The adsorption mechanism follows Langmuir adsorption isotherm model and found that the protective film appears on copper is the most persistent, followed by mild steel and lastly aluminium 1050 (Sabet Bokati & Dehghanian, 2018). Raviprabha and Ramesh (2019) explained that the adsorption process of an organic inhibitor on the metal surface through chemisorption. The inhibition efficiency can be found as high as 94.1% at low inhibitor concentration.

In acidic environments, Nnaji et al. (2019) suggested that benzothiazole and its derivative shield the aluminium from the attack of Cl^- (from acid) by adsorbing on aluminium surface and form a protective barrier. The inhibition efficiencies range from 28.2 -76.1% in the presence of little inhibitor concentration range of 2 to 10 μM. Ishwara Bhat and Alva (2011) in the study of aluminium corrosion inhibition in an acid medium by an anti-emetic drug stated that the inhibitor intercepts the corrosion process of aluminium by adsorption. The inhibitor adsorbs strongly on the aluminium surface and follows the Langmuir adsorption isotherm model which hinders the dissolution reaction in a corrosive medium. Another literature that uses drug as corrosion inhibitor in the study of aluminium corrosion behaviour in HCl is by Abdallah et al. (2019) and Chen et al. (2021) using tramadol and Vitamin B1 respectively. The authors suggested that benzene rings in the molecular structure of the drug inhibitors adsorbed on the aluminium surfaces, forming a protective film and retard corrosion process. The protective layers were observed under SEM and the adsorption mechanism follows the Langmuir adsorption isotherm. They exhibit high corrosion inhibition efficiency at optimum temperature and pH. For alkaline solution, the alkoxnium inhibitor exhibits good corrosion inhibition on aluminium. The inhibition mechanism was found to obey Langmuir isotherm. The inhibitor does not adsorb well in acidic solution because of the induced repulsion between positive alkoxnium inhibitor in acidic electrolyte and the positive sites produced on aluminium surface. The induced repulsion decreases the adsorption of the inhibitor through anodic process (Hassan et al., 2018). The corrosion inhibition adsorption mechanism can be proved by Langmuir and other adsorption isotherms. In this study, no adsorption isotherm is used to investigate the corrosion inhibitor behaviour due to time constraints. The corrosion inhibition mechanism will be explained using the potentiodynamic polarisation measurement which will be discussed in Section 2.2.7.

2.2.6 Inhibitor evaluation

The degree of surface coverage (θ) on the metallic surface is intrinsically linked to excellent corrosion inhibition as a thick and stable adsorptive layer serves as a greater barrier against aggressive media. Inhibitor efficiency, IE can be a good indicator of surface adsorption extent. IE can be determined according to the following correlation:

$$\mathrm{IE\%} = \frac{\mathrm{I_o} - \mathrm{I_i}}{\mathrm{I_o}} \times 100 \tag{13}$$

Where I_o is the corrosion current density without inhibitor, I_i is the corrosion current density with inhibitor, I_o and I_i can be determined using any of the standard corrosion techniques (El-Lateef et al., 2019; Prakashaiah et al., 2018) . Any unit of corrosion rate can be used considering the units are consistent throughout all tests.

2.2.6.1 Inhibition in acidic solution

Pickling, surface cleaning, gas/oil well acidizing, and electrochemical etching of metals and alloys usually contain hydrochloric acid in the solutions (El-Lateef et al., 2019). In acidic solution, the common choice of inhibitors often composed of a head group that attaches to the surface, and a more hydrophobic tail group that reaches out into the electrolyte as illustrated in Figure 2.7.

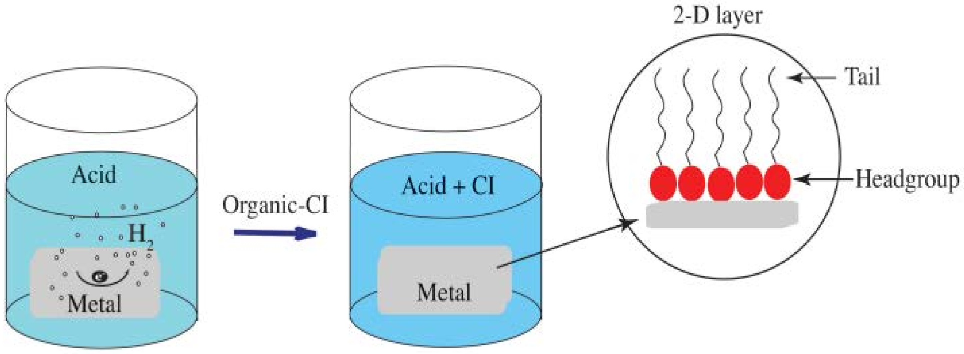

Figure 2.7: Interaction of corrosion inhibitor with a metallic substrate in acidic solution, a 2-D monolayer is formed.

Organic inhibitors that consist of heteroatoms like S, N, and O, and pi electrons from aromatic rings, double and triple bonds are aggressive and adsorb easily on metal surface in acidic environments.

Organic inhibitors have a threshold concentration below which they stop inhibiting and start stimulating. It is important to constant monitoring of inhibitor concentration in acidic solution when using organic inhibitors to ensure it does not fall below its critical value. Under some circumference of acid solution, corrosion is associated by strong hydrogen diffusion. It has been shown that metal dissolution inhibitors do not always reduce hydrogen uptake, and in certain situations, they may even enhance it (Monticelli, 2018). Incorrect choice of organic inhibitors instigating the corrosion and hydrogen penetration into the metal. The initial stage of the inhibition mechanism in strong acid media is the adsorption of inhibitors onto the metal surface. The nature and surface charge of the metal, molecular structure of the inhibitor, and type of aggressive electrolyte influence the adsorption process. Aluminium is prone to corrode in strong acid such as hydrochloric acid compared to sulphuric acid. According to Loto and Babalola (2019), hydrochloric acid contains Cl^- anions which is aggressive on metal surface. It adsorbs on the surface of the protective oxide film due to the net positive charge on the metal surface in the electrolyte. This adsorption leads to concentration of chloride ion at specific regions on the metal surface resulting the formation of local anode sites. Nwanonenyi et al. (2019) studied the effect of hydroxypropyl cellulose as corrosion inhibitor on aluminium in acidic environments, stated the aluminium exhibit higher resistance to dissolution in sulphuric acid than in hydrochloric acid due to pits formed on the metal surface by Cl^- ions encouraged faster corrosion rate. The inhibition efficiency improved with increase in corrosion inhibitor concentration, but its long-term viability was affected with increase in temperature (Jessima et al., 2020). Abdallah et al. (2019) explained that organic inhibitor in 1M HCl solution mainly act as anodic than cathodic using data obtained by potentiodynamic polarisation. The work presented by Chen et al. (2021) also found that organic inhibitor retards the corrosion on aluminium in hydrochloric solution using anodic reaction while cathodic reaction only plays a minor role. Hence, organic inhibitors commonly act as a mixed-type inhibitor which is anodic dominant.

2.3 Electrochemical Techniques

Electrochemical techniques are often used to assess corrosion, and there are several good textbooks available that cover the fundamental electrochemical concepts in depth (Kenney & Hwang, 2009; Pourbaix, 1991; Szklarska-Smialowska, 1991).

2.3.1 Open Circuit Potential

Open circuit potential (OCP) is the constitutive potential (E_{corr}) of a corroding electrode in an electrolyte. At this potential, the half reactions at both anode and cathode take place simultaneously, $I_a=I_c$. Other terms used to describe OCP are ‘free corrosion potential’ and ‘mixed corrosion potential’. The limited information obtained from simply measuring OCP can be used to evaluate the relative likelihood of corrosion. A more positive value often indicates that a metallic substrate is less prone to electrochemical dissolution, but there are cases where a more positive OCP value is due to a rise of cathodic reaction rate. OCP can also be evaluated as a function of a corrosion inhibitor, which provides insight into how a system (corrosion) responds to a disturbance.

2.3.2 Potentiodynamic polarization

Potentiodynamic polarization (PDP) is widely used method to study corrosion. It elucidates the nature of corrosion process by polarising a sample away from OCP for more direct understanding of anodic and cathodic processes. A positively polarised sample, the measured current is related to anode activities. In a sample polarised in negative direction, current is governed by cathodic activities and anodic activities become insignificant. PDP measurements are typically taken by scanning the sample potential from below to above E_{corr}, while the anodic and cathodic branches may be acquired individually. The spectrum of potential scan is approximately several hundred millivolts. As shown in Figure 2.8, data is generally represented as log of current density against potential (Szklarska-Smialowska, 1991).

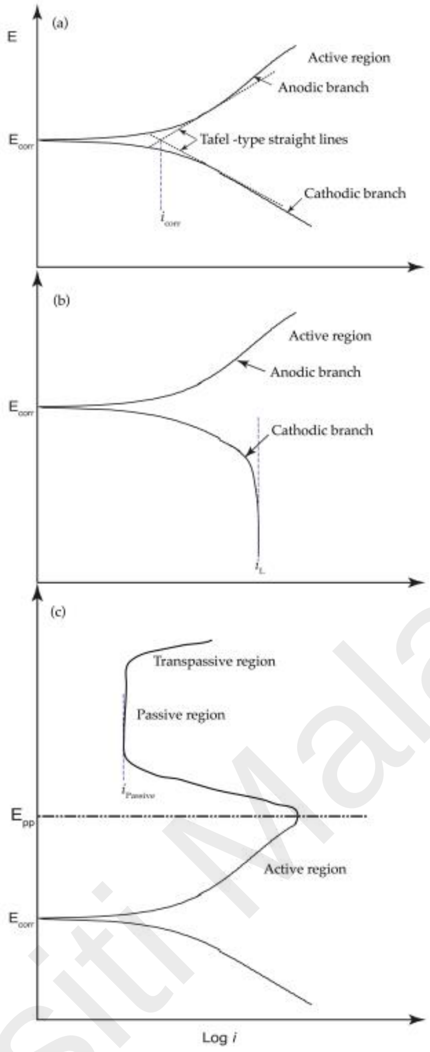

Figure 2.8: Schematic diagrams of PDP curves. (a) Activation controlled anodic/cathode processes, with Tafel extrapolation approach to estimate I_{corr} and E_{corr}. (b) Cathodic branch curve which indicates a diffusion-limited process with constant/limiting current. (c) Anodic branch curve that anticipates passivation of substrate.

The polarization curve shows a profile that indicates activation-controlled anode/cathode processes (linear areas as potential is polarised away from E_{corr}, corrosion current density I_{corr}, thus corrosion rate can be calculated using Tafel extrapolation of the anodic and cathodic branches. This approach presupposes Tafel behaviour in the anodic and cathodic reactions. Butler-Volmer equation expresses the dependency of current upon potential (Szklarska-Smialowska, 1991):

$$E = a + bLogI$$

(14)

where a and b (referred to as Tafel slope in mV/decade unit) are constants. The corrosion current rises at potentials greater than E_{corr} (anodic branch), reaches a peak passivation potential (E_{PP}), and then decreases. As the potential is raised, the low corrosion current is maintained until the film is broken down owing to transpassivity/pitting (Usman et al., 2020). A shortcoming of the Tafel extrapolation technique to determine corrosion rate is when a relatively large potential that fluctuates from E_{corr}, can change the sample surface. The sample should be reprepared using initial procedures when the measurement is to be repeated. This is to achieve stability in electrolyte and eventually reach steady E_{corr}.

A PDP curve can provide additional information on interfacial electrochemistry, including the existence of diffusion-controlled processes and passivation of substrate. The presence of corrosion inhibitor may shift the initial E_{corr} without inhibitor by interfering the anodic, cathodic or both reactions. Figure 2.9 demonstrates these changes reflected in PDP curves (Pedeferri, 2018b).

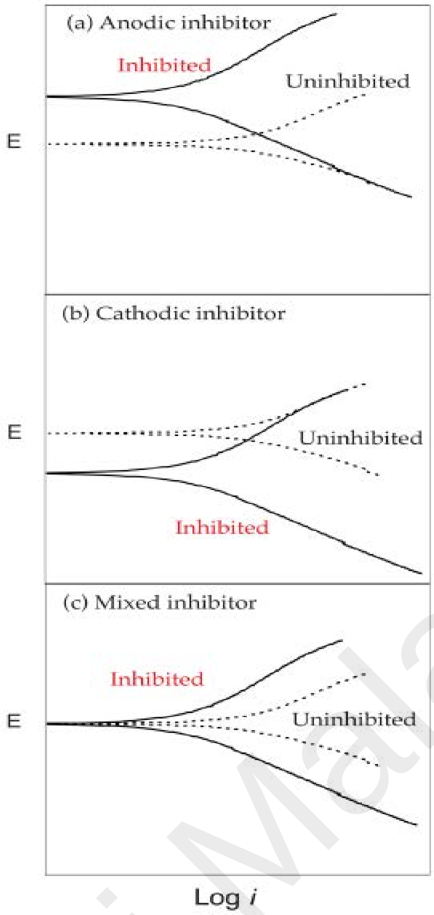

Figure 2.9: Addition of anodic, cathodic, or mixed inhibitors change the uninhibited PDP curves.

The potentiodynamic polarisation instrument will be discussed in Chapter 3: Methodology.

2.3.3 Corrosion Rate Measurement

Corrosion rate can be calculated from the corrosion current provided in Tafel plot, in mm/year (mmpy), using the following equation:

$$mmpy = I_{corr} \times A \times \frac{1}{\rho} \times \varepsilon$$

(15)

Where I_{corr} is the corrosion current density in Amps/cm^2, A is the combination of several conversion terms and is 1.2866 x 10^5 (Coulumbs.cm.years), ρ is the metal density in g/cm^3, and ε is the equivalent weight in g/equivalent. Equivalent weight is the metals weight in gram is divided by the number of electrons in metal's anodic half reaction. The density of 5052 aluminium alloy is 2.68 g/cm^3.

2.4 Scanning Electron Microscopy

Scanning electron microscopy (SEM) scans the surface of the sample with a low-energy beam of electrons and creates image for the analysis. It has short probe electrons' wavelength which produce substantially great spatial resolution. The diffraction limit is low at approximately 1000 kV accelerating voltage of and 0.004 nm wavelength. SEM components include electron source/gun, electron lenses, sample stage, detectors for all signals of interest, display/data output devices. A schematic diagram of the essential components and modes of operations of SEM is shown in Figure 2.10.

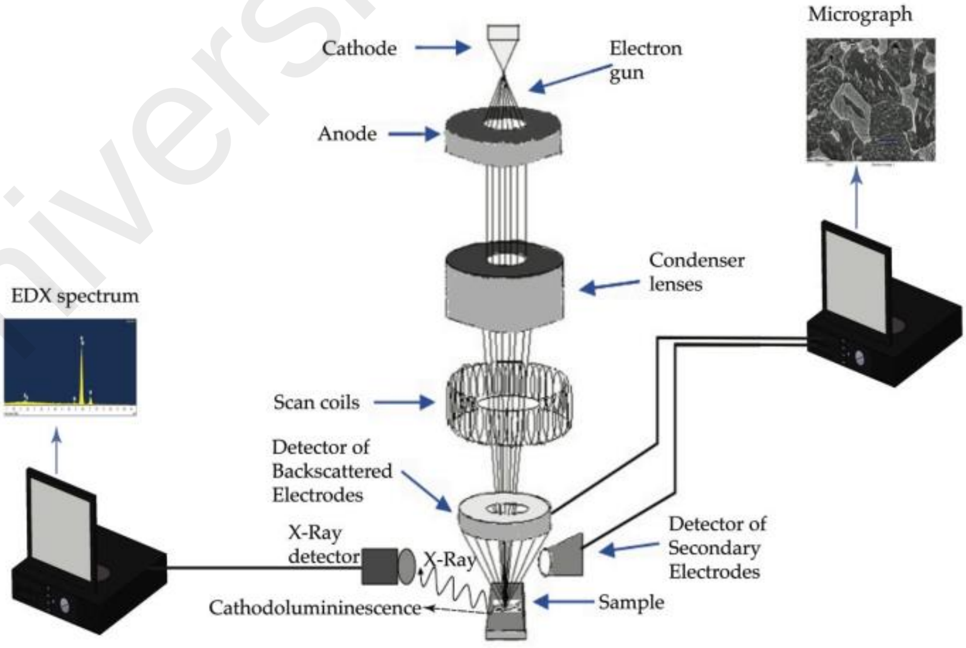

Figure 2.10: SEM main components, including generated signals

SEM can show the difference of the morphological appearance of the metal surface with and without corrosion inhibitor. Figure 2.11 displays the structure of zinc surface with the absence and presence of the chondroitin sulphate inhibitor in ammonium chloride solution (Singh et al., 2020).

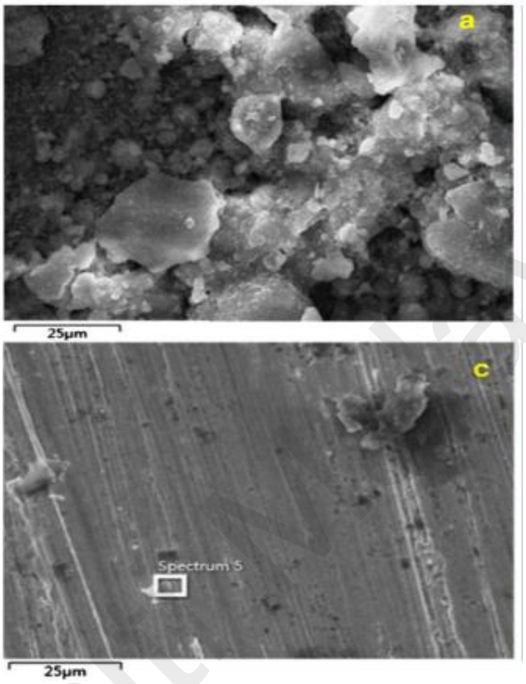

Figure 2.11: SEM image without CS (above) and with CS (below).

It can be seen that the sample with inhibitor has smoother surface compared to the sample without inhibitor.

2.5 Optical Microscope

Most optical microscopes are compound microscopes, which have at least two lenses. Lenses are curved pieces of glass or plastic that magnify objects and make them look larger than they really are. The compound microscope provides two levels of magnification. The initial magnification is produced when light from a mirror is reflected up through the specimen and into the powerful objective lens. The eyepiece lens, which functions as a basic magnifying glass, then magnifies the image generated by the objective lens. The enlarged image can be seen via the eyepiece lens (Homborg et al., 2022).

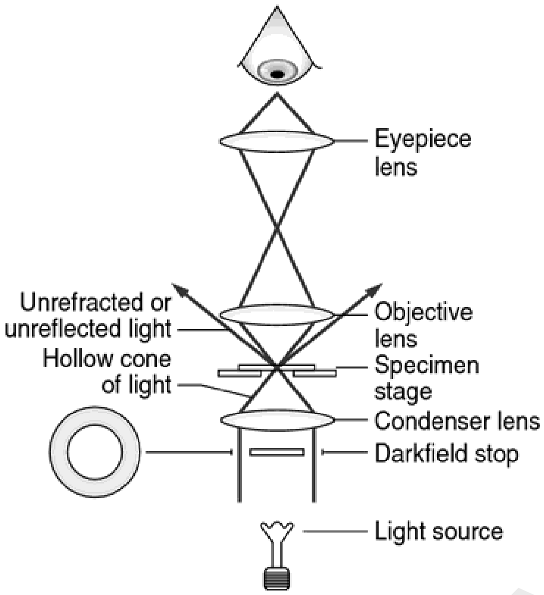

Figure 2.12: The optical microscope

Figure 2.13 - 2.14 shows the images produced from optical microscope before and after corrosion respectively.

Figure 2.13: Optical morphology of sample A before corrosion.

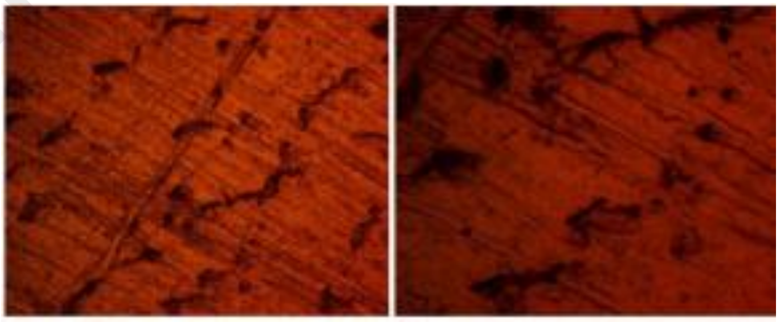

Figure 2.14: Optical morphology of sample A after corrosion.

The surface deterioration of metal from optical microscopy is appeared after the corrosion as the sample is slightly etched by the environment (Loto & Babalola, 2019).

2.6 Sulphate-containing compound as organic corrosion inhibitor

Sulphate is a polyatomic anion with the empirical formula SO_4^{2-} is consisted of S and O atoms, with 149 pm S-O bond length (Coulson, 1969). S have low electronegative value which offers strong coordinate bonding with metallic surface and produce high efficiency in preventing corrosion of metals (Verma et al., 2018). In view of this, several sulphate-containing compounds have been tested as corrosion inhibitor for metals and alloys in different electrolyte environments.

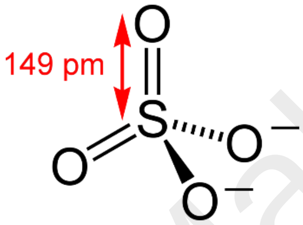

Figure 2.15: The chemical structure of sulphate with ionic bonding.

2.6.1 Inhibition on aluminium and other metals/alloys

Hassan et al. (2018) studied the inhibition property of anionic polyelectrolyte chondroitin-4-sulfate (CS) polysaccharide on corrosion of aluminium in hydrochloric acid employing gasometrical and weight-loss techniques. They found that CS inhibiting behaviour is more effective in alkaline environment compared to in acidic environment with increasing concentration. The CS adsorbed on Al metal surface and was found to obey Langmuir isotherm.

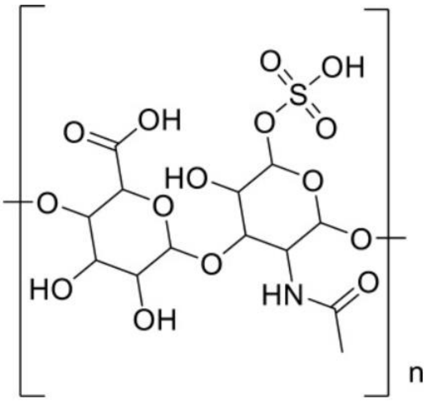

Figure 2.16: Molecular structure of CS

CS also was used in the study of mild steel corrosion in 1 M HCl by Basik and Mobin (2020) in the later year. It was discovered that the inhibitor efficiency of CS could reached as high as 94% at 500 ppm concentration at 333K. The analysis of PDP shows that compound acts as a mixed-typed inhibitor with anodic dominance. The surface characterisation studies dictates that the presence of additional peaks of S and absence of Cl peak confirms that heteroatom is responsible for inhibition process. Density-functional theory analysis carried out for CS molecules provides insight of neutrophilic and electrophilic attack on metal surfaces, support the contribution of heteroatom in enhancing the corrosion resistivity of inhibitor on metal surface. SEM images justify the presence of inhibitor reduce the corrosion and smoothened the surface of the specimen. The corrosion inhibiting property of CS was also investigated on zinc-carbon battery in 26% ammonium chloride solution by (Singh et al., 2020). The nature of CS adsorption is mixed typed with cathodic dominant. The inhibition efficiency reaches 98.9% at 200 mg/L inhibitor concentration in 26% NH_4Cl solution at 308K. CS adsorbed on the metal surface and formed thicker protective film layer on the metal surface. The thickness of protective film increases when the concentration of CS in the electrolyte increases. SEM, energy dispersive X-ray spectroscopy, and X-ray photoelectron analysis supports the presence of CS adsorbed film over the metal surface.

It was observed that the adsorption follows the Awady adsorption isotherm model. It can be concluded that the concentration of inhibitor is not the same in different environment. The same type of inhibitor could have different optimum conditions depending on the pH and temperature of electrolyte, and type of metal to maximise its functionality in inhibiting corrosion.

Song et al. (2021) discussed that sodium dodecyl sulphate (SDS) adsorbed on Mg-8Li-3Al alloy surface in NaCl solution and created a dense and uniform protective layer. The barrier reduced potential difference between cathodic and anodic phases and inhibit the corrosion from happening. The polar sulphate of SDS adsorbed with the matrix of metal and reached 89.1% efficiency inhibiting corrosion although there was a few severe corrosion sites occurred on the surface. In the recent study by Koundal et al. (2022), SDS has the ability to minimise corrosion on mild steel in NaCl solution, but the inhibition is more effective with the addition of imidazolium ionic liquid (DMImCl). Hydrophobic chains of DMImCl attract the hydrophobic end of SDS, which increases the electron-donating ability of the molecules to the surface of positively charged mild steel. Sulphate-compound inhibitor can be optimised its efficiency by mixing with another compound that can help to enhance its electron donating characteristic. Nonetheless, mixing two or more inhibitors will require a long and complicated research. Sodium lauryl sulphate was used to modify chitosan which is an excellent corrosion inhibitor for a mild steel in 1 M HCl, to further improve its corrosion inhibition behaviour. The modified inhibitor has a long hydrophobic alkyl chain called sodium lauryl sulphate modified chitosan (SLC). SLC reduced the corrosion of the mild steel by preventing the access of water molecules to the metal surface because of its Van der Waals forces between the aliphatic chains. (Jessima et al., 2020). This inhibition mechanism involved in both anodic and cathodic reactions. Mixed-typed inhibitor has higher efficiency to suppress corrosion on metal compared to anodic- or cathodic-dominant inhibitor.

The added heteroatoms such as oxygen and nitrogen atoms of the chitosan increased the adsorption of the inhibitor on the metal surface. When zinc sulphate is added into an aggressive sodium chloride solution, the polarization curves of mild steel after 1 hour of immersion depicts that the presence of zinc sulphate decreases the corrosion current density. The value of E_{corr} shifted toward more negative value, thus zinc sulphate exhibit cathodic inhibition mechanism. It retards the oxygen reduction reaction at active cathodic sites. Thermodynamic studies determined that the adsorption process of inhibitor obeys the Langmuir isotherm (Ismail et al., 2019). The sulphate-containing compound can be used to mix with polymer or surfactant to boost the corrosion inhibition efficiency on metals and alloys. These inhibitors worked synergistically and adsorbed on metal surface, creating protective film to stop metal from corroding (Ismail et al., 2019). When two compounds are applied onto the metal surface, there are two kinds of adsorption mechanism, competitive and cause antagonistic effects. The ability of single sulphate-containing compound in increasing the strength of protective layer is on par to the mix compounds inhibitor, which makes sulphur-containing compound alone is reliable to resist corrosion. A molecular perspective of iron corrosion driven by chloride and sulphate is studied by Chen et al. (2022). The authors claimed that anions that have negative energy values could easily adsorb on the metal surface. Figure 2.17 shows the interaction of sulphate is stronger than chloride, where the S atom is located at the hollow site of the metal and exhibit higher negative adsorption energy compared to chloride. The sulphate attack on metal surface is similar to chloride attack which is belong to localised corrosion which favours pitting on the metal surface.

The individual presence of chloride and sulphate in an electrolyte promotes corrosion on metal surface. Yet, when chloride and sulphate exist together in an electrolyte, the two ions mutually compete and weaken the interaction with the metal surface, in results low corrosion rate on metal.

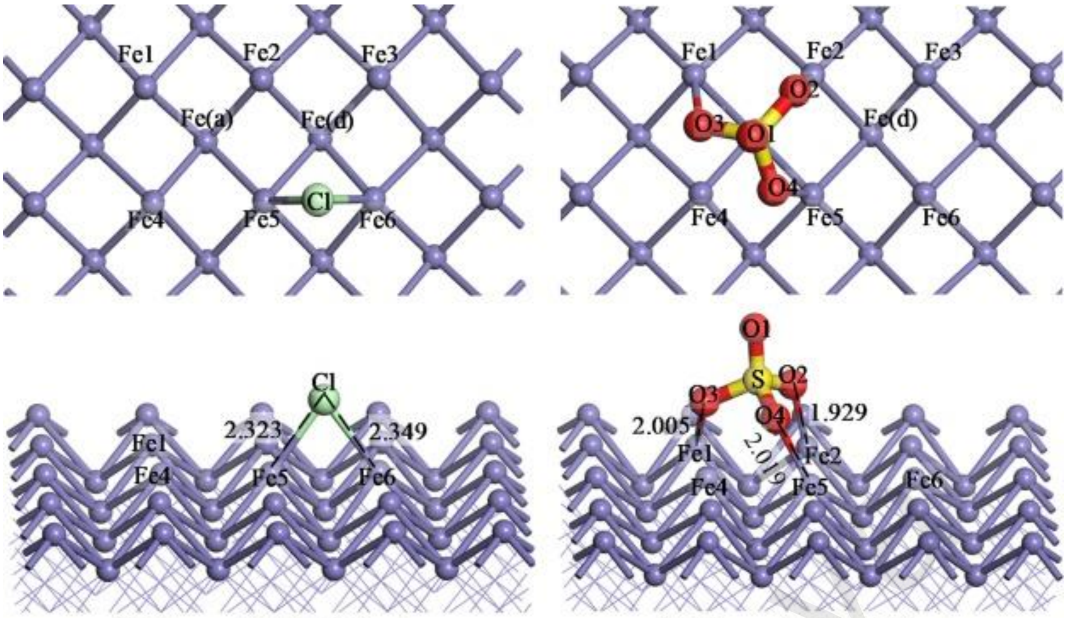

(a) $E_a = -457.726$ kJ/mol (b) $E_a = -736.183$ kJ/mol

Figure 2.17: The adsorption configuration of chloride and sulphate on metal surface. The top and side views of the (a) Cl^- (b) SO_4^{2-} on metal surface.

2.6.2 Sodium sulphate as corrosion inhibitor

Sodium sulphate is a white crystalline solid of formula Na_2SO_4. It is highly soluble in water and can be found in glass and paper production, and in detergents' compound. When dry, it has no action on aluminium, but can cause mild, consistent attack on aluminium in solution at ambient temperature. In a solution of 10 % sodium sulphate, the dissolving rate of aluminium is around of 0.01 mm each year (Vargel, 2004). Bai et al. (2021) found that the binding energy of sulphate ion to iron is 169.2 eV. When the concentration of sodium sulphate rises from 0 to 2 g/L in saturated steam, the iron corrosion products increase from 43.4% to 56.2%. A small amount of sodium sulphate dissolved in saturated steam has effect on the corrosion behaviour of iron. Rodič et al. (2019) evaluated the corrosion performance of sodium sulphate on aluminium in a solution contains cerium acetate. It is examined that sodium sulphate inhibits the corrosion on aluminium by forming more compact and durable film on aluminium surface.

The corrosion mechanism is confirmed by the electrochemical technique, which sodium sulphate acts as anodic inhibitor. In another study done by Rodič et al. (2021) to focus on the behaviour of sodium sulphate attending the cerium acetate presence. Cerium acetate inhibit corrosion at low temperature by forming precipitation on the surface but at high temperature, the precipitate is formed in the solution which promotes faster corrosion process. The author stated that when sodium sulphate is added into the solution containing cerium acetate, sulphate ions decreased the I_{corr} and I_c by suppressing the undesired precipitation of cerium and increase the conversion of Ce^{3+} into Ce^{4+}, in result retard the corrosion process of the aluminium surface. Sulphate ions act as grain refiner for inhibitor growth and enhance the corrosion protection of AA7075-T6 and AA2024-T3 by adsorbing on the metal surface or the incorporation into the formed film. The formation of barrier film is denser at lower temperature compared to high temperature. (Rodič et al., 2021; Rodič et al., 2019). There are only few literatures that discussed the mechanism of sodium sulphate as corrosion inhibitor. Sodium sulphate could induce corrosion or slow down corrosion depending on the presence of other compounds, pH, and temperature of the electrolyte. For a novel approach of this project, sodium sulphate is used to study the effects of sulphate on inhibiting corrosion of aluminium alloy in variety acidic environments.

CHAPTER 3: METHODOLOGY

3.1 Aluminium specimens

The flat 5052 aluminium alloy specimens were cut into 1 x 1 -inch sized from metal sheets. The surface of the specimens was prepared by rubbing with 400, 600, 800 and 1200 grit silicon carbide abrasive paper by hand then polished with 1 and 3 μm diamond polishing paste using polishing machine until each surface became smooth and mirror finished.

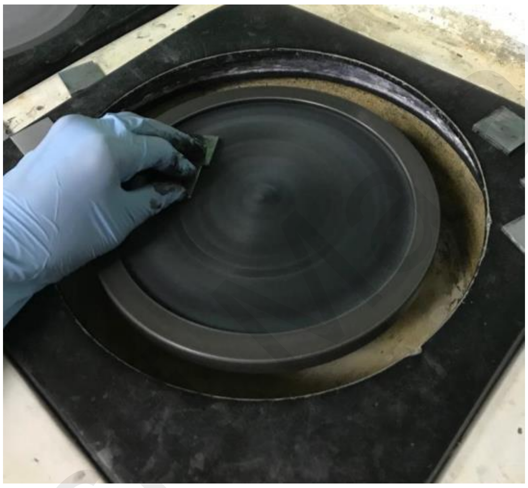

Figure 3.1: The aluminium alloy specimen is polished using polishing machine in laboratory.

During the grinding and polishing processes, the gloves must be replaced with new ones every time using different grit of abrasive paper. The specimens were degreased using acetone and cleaned in ultrasonic cleaner for 5 minutes and finally dried at room temperature. The polished samples were kept separately in a zip-lock bag with silica gel. The properties of the 5052 aluminium alloy specimens are: 5.585 g of weight, 1.186 g of equivalent weight, 2.680 g/cm^3 of density, ρ and 6.453 cm^2 of surface area. These values are important to calculate the corrosion rate of aluminium.

3.2 Electrolytes preparation

Hydrochloric acid used was the highest available purity (>90%). The pH of the electrolyte was altered by adding concentrated 1 M NaOH into 1 M HCl solution in a beaker under a fume hood, measured using pH meter. Three different pH of 2, 4 and 6 were prepared in different beaker and the solutions are kept in glass containers. Distilled water was used for pH 7 electrolyte. Sodium sulphate powder was weighted based on the desired concentrations which are 200, 400 and 600 mg/L. The inhibitor is diluted using distilled water separately in a beaker until there is no precipitation. The inhibitor solution is then mixed into the different pH electrolytes.

Figure 3.2: The pH reading of the prepared electrolyte using pH meter.

3.3 Potentiodynamic polarization test

The BioLogic SP-150e was the electrochemical workstation used to analyse the corrosion process happened on the aluminium surface. PDP measurements were carried out in 1L glass cell using a conventional three-electrode system comprising 5052 aluminium alloy for the working electrode, platinum electrode as the auxiliary electrode, and saturated calomel electrode (SCE) as the reference electrode. The area of the working electrodes exposed to electrolyte was 1 inch^2.

The open circuit potential was measured in a pH 2, pH 4, pH 6, and pH 7 solutions with sodium sulphate concentrations of 200, 400, and 600 mg/L and a blank system without sodium sulphate. The data were processed using EC-Lab software to analyse the corrosion behaviour of the system. The measured current represents the rate of corrosion on the working electrode in term of current per unit area, which is referred as current density.

Figure 3.3: Three-electrodes system potentiodynamic polarisation setup

The extrapolation of the cathodic and anodic branches of Tafel plot to potential indicated the corrosion current density of the studied electrodes (El-Lateef et al., 2019). During polarisation, placing the reference electrode on the test electrode surface is the best technique to assess test electrode potential. Placing a reference electrode on the surface of a test electrode would impede the passage of ionic current to/from the test electrode at the point of contact and might also produce pitting corrosion. to avoid test electrode blockage (also known as shadowing), the reference electrode must be positioned at a distance, generally two reference electrode diameters away from the test electrode surface.

To ensure the reliability of the electrochemical PDP data, the experiments were carried out using a fresh solution and clean set of electrodes at ambient temperature to avoid contamination.

3.4 Optical microscopy

The clean samples were plcaed onto the sample stage underneath the objective lense. The sample stage was adjusted using the outer and inner knob in z-direction until the sample can be focussed thourgh lens. The sample is observed using the objective lens until the desired magnification. In this project, 5x, 10x, 20x and 50x magnification lens were adjusted from the lowest to highest, to find the best morphological image of the sample.

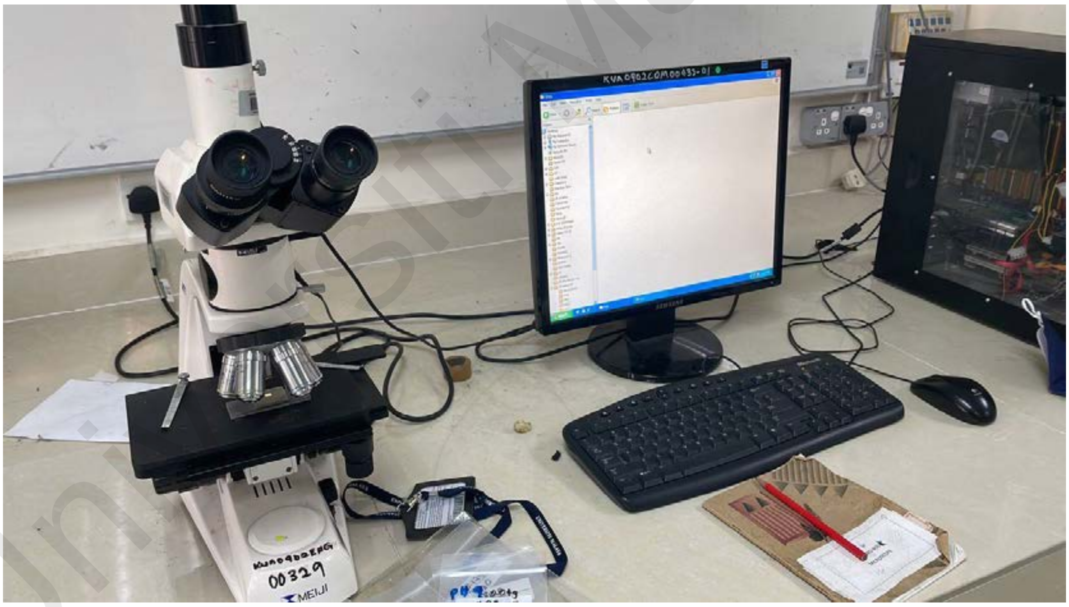

Figure 3.4: The setup for optical microscope in laboratory.

The morphological images appeared on the computer screen via microscopy image and analysis software.

3.5 Weight loss measurement

The samples were weighed using electronic measuring scale before immersed into acidic electrolytes in a closed-lid container separately. The samples were then removed, cleaned, and reweighed after seven days. The weight difference/loss, Δw was recorded, and the values were used to calculate corrosion rate. Corrosion rate for this method is calculated using the following formula:

$$mmpy = 87.6\ x\ \frac{\Delta w}{\rho AT} \tag{16}$$

Where T is the immersion period (h). Multiply mmpy with 39.37 to convert into mils/y.

CHAPTER 4: RESULT AND DISCUSSION

The influence of sulphate on inhibiting corrosion of aluminium alloy was investigated by electrochemical experiments. Corrosion parameters were obtained using cathodic and anodic potential against current density characteristics in the Tafel potential area.

4.1 Potentiodynamic Polarization

4.1.1 Tafel plots analysis

Figure 4.1 – 4.3 depicts the polarisation curves of aluminium in acidic electrolytes while figure 4.4 depicts the polarisation curves of aluminium in neutral electrolyte.

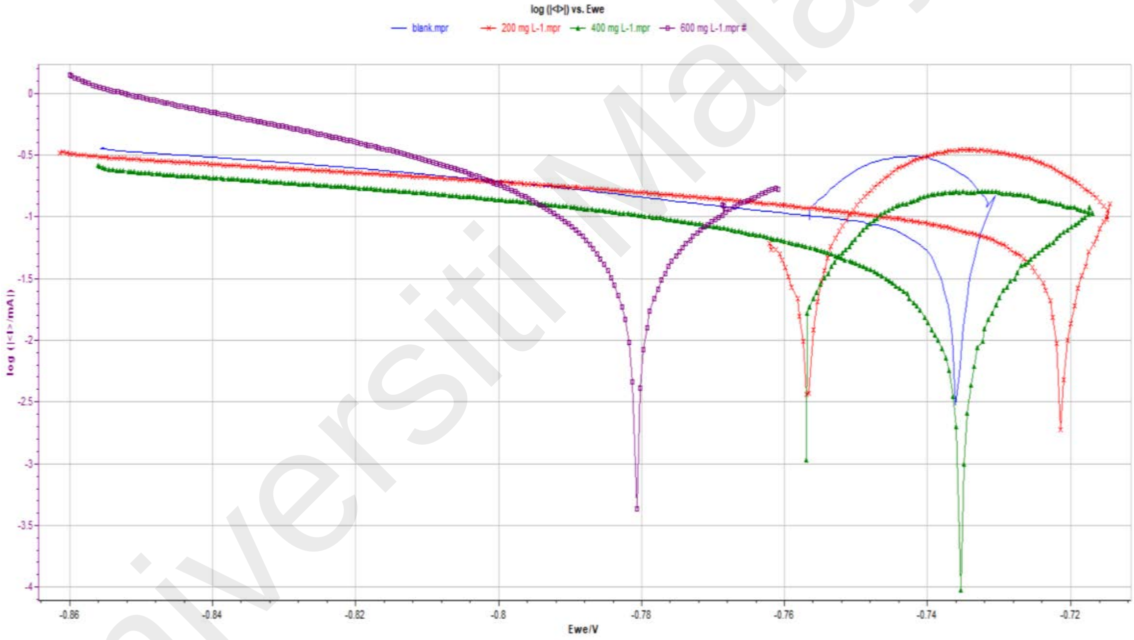

Figure 4.1: Potentiodynamic polarization curves for 5052 aluminium alloy in a pH 2 environment at atmospheric condition.

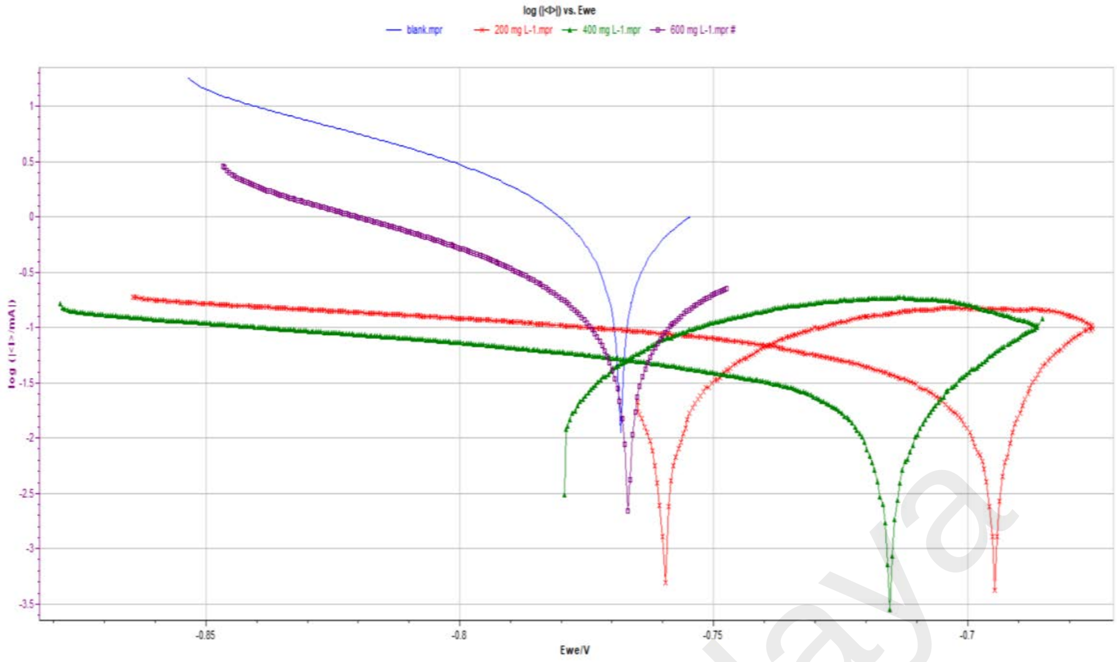

Figure 4.2: Potentiodynamic polarization curves for 5052 aluminium alloy in pH 4 environment at atmospheric condition.

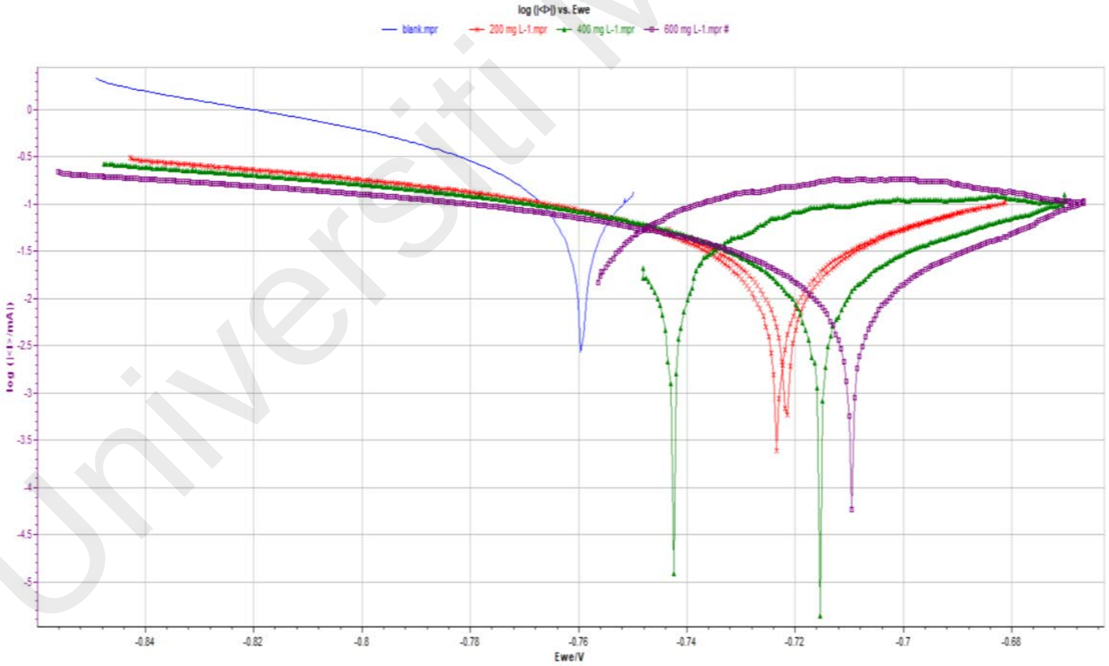

Figure 4.3: Potentiodynamic polarization curves for 5052 aluminium alloy in pH 6 environment at atmospheric condition.

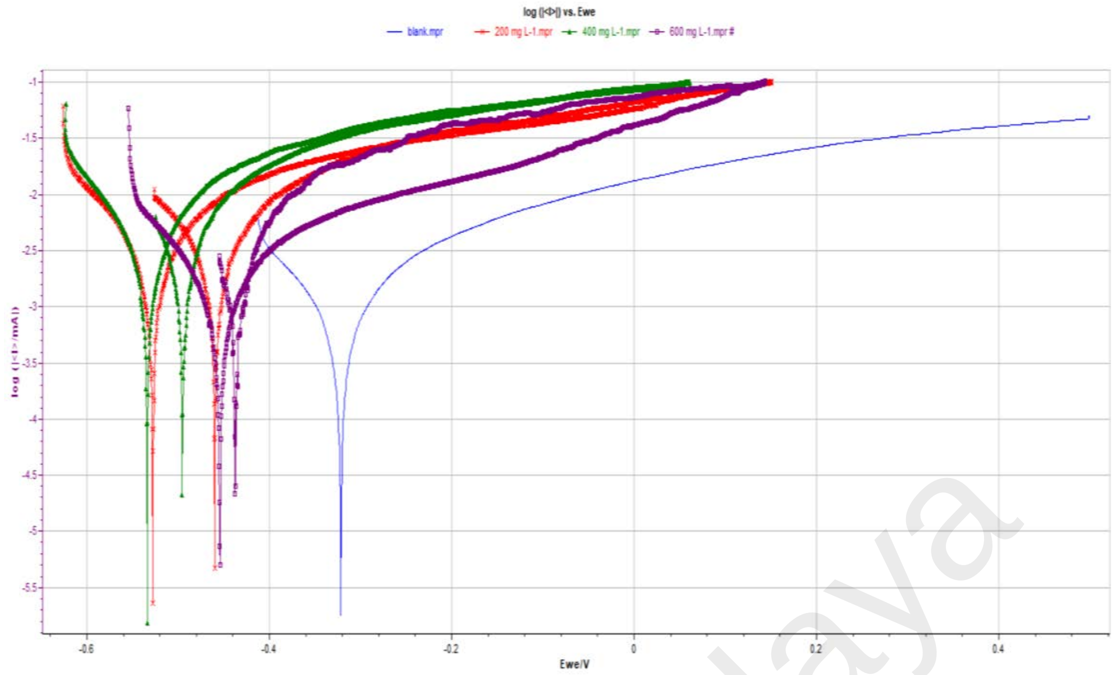

Figure 4.4: Potentiodynamic polarization curves for 5052 aluminium alloy in pH 7 environment at atmospheric condition.

The polarization plots (potential against log current) in figure 4.1 – 4.3 represent the corrosion results from the immersion of aluminium in acidic electrolyte in the absence and presence of sodium sulphate at different concentrations. In the presence of sodium sulphate, the polarisation curves of the inhibited samples reveal that a large effect to the anodic branch suggestive of passivation occurred in the presence of the inhibitor. The overall anodic behaviour of the curves is showing reverse scan in positive hysteresis, where the value of log I in reverse scan is greater than the forward scan. Positive hysteresis gives information such as passive region is damaged with the residence of Cl^- in hydrochloric solution or SO_4^{2-} in sodium sulphate, and that pits will continue to grow even in the presence of inhibitor. There is a steep rise into anodic current density from the point of open circuit. The potential at this peak is also known as the repassivation potential in transpassive region of potentiodynamic curves. The corrosion current density can be estimated by extrapolating the reverse anodic scan to an intersection with the corresponding OCP curve cathodic branch (table 4.1).

Both anodic and cathodic branches at 200, 400 and 600 mg/L concentrations sweep into lower log I values than the uninhibited sample. The log I values for OCP at all concentrations were also lower than uninhibited sample and the most pronounced fall of log I was observed at 400 mg/L concentration. The cathodic branch of inhibitors shows similar behaviour and mainly became steeper than the uninhibited sample except for 600 mg/L concentration in pH 4.

Based on figure 4.1, the OCP of the 200 mg/L concentration shifted to more positive while the OCP of the 600 mg/L inhibitor concentration shifted to more negative. The OCP of the 400 mg/L concentration almost identical to the uninhibited sample in pH 2 electrolyte. Figure 4.2 and figure 4.3 display that all inhibited samples have OCP that shifted to more postive than the blank sample pH 4 and pH 6 electrolytes.

Figure 4.4 shows the overall inhibited samples undergone negative hysteresis thus, pitting is not expected to occur on aluminium alloy in neutral solution. OCP of uninhibited sample was more positive than the inhibited solutions. Generally, neutral electrolyte have less negative OCP compared to acidic electrolytes without inhibitor which in this case, the OCP for pH 7 is -0.36V while for pH 2, 4 and 6 is in the range between -0.73V to -0.78V. The subtle cathodic branches in Tafel plot express the hydrogen evolution process is neither activation nor diffusion controlled (Cen et al., 2019). This observation indicates that SO_4^2 affects the electrochemical actions on aluminium in acidic as corrosion inhibitor, and not much effect in neutral environments. The retardation of corrosion on aluminium could be affected with the presence of Cl^- in the electrolyte.

4.1.2 Other corrosion parameters

The electrochemical parameters determined from the linearly fitted of polarization curve in the Tafel zone include corrosion current density (I_{corr}), corrosion potential (E_{corr}), anodic (β_a), and cathodic (β_c) Tafel slopes and corrosion inhibition efficiency (IE%).

The extrapolation of the cathodic and anodic Tafel lines to the E_{corr} yielded the I_{corr} values for the examined aluminium alloy with and without the inhibitor respectively. The relative magnitudes of β_a and β_c were used to classify the manner of inhibition as predominantly anodic or cathodic.

Table 4.1: Polarization parameters for 5052 aluminium alloy in various pH environments in the absence and presence of different inhibitor concentrations.

pH of environment	Conc. of inhibitor (mg/L)	I_{corr} (μA cm^{-2})	E_{corr} (mV)	β_a (mV dec^{-1})	β_c (mV dec^{-1})
2	Blank	153.4	751	15.00	275.4
	200	123.2	747	13.40	273.1
	400	81.63	743	30.70	235.5
	600	94.23	770	37.20	79.40
4	Blank	85.48	753	15.70	69.60
	200	68.00	712	10.70	204.2
	400	66.31	714	24.30	221.1
	600	69.91	736	62.00	248.2
6	Blank	160.9	774	23.90	38.80
	200	77.60	732	27.60	35.60
	400	52.21	757	33.30	68.80
	600	121.7	760	49.60	273.6
7	Blank	1.009	380	293.6	43.10
	200	1.633	580	328.2	34.30
	400	1.850	594	294.3	21.60
	600	1.473	523	276.3	24.50

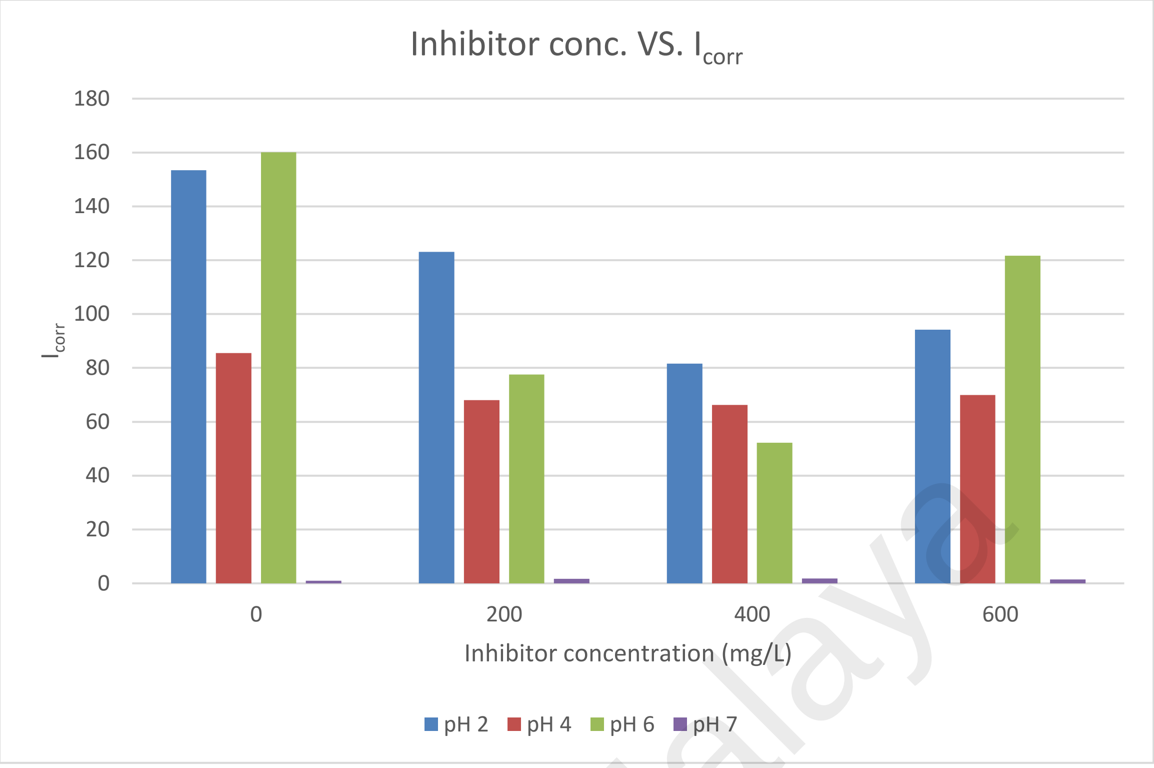

Figure 4.5: Corrosion current density against concentration of sodium sulphate inhibitor on aluminium alloy in different pH environments.

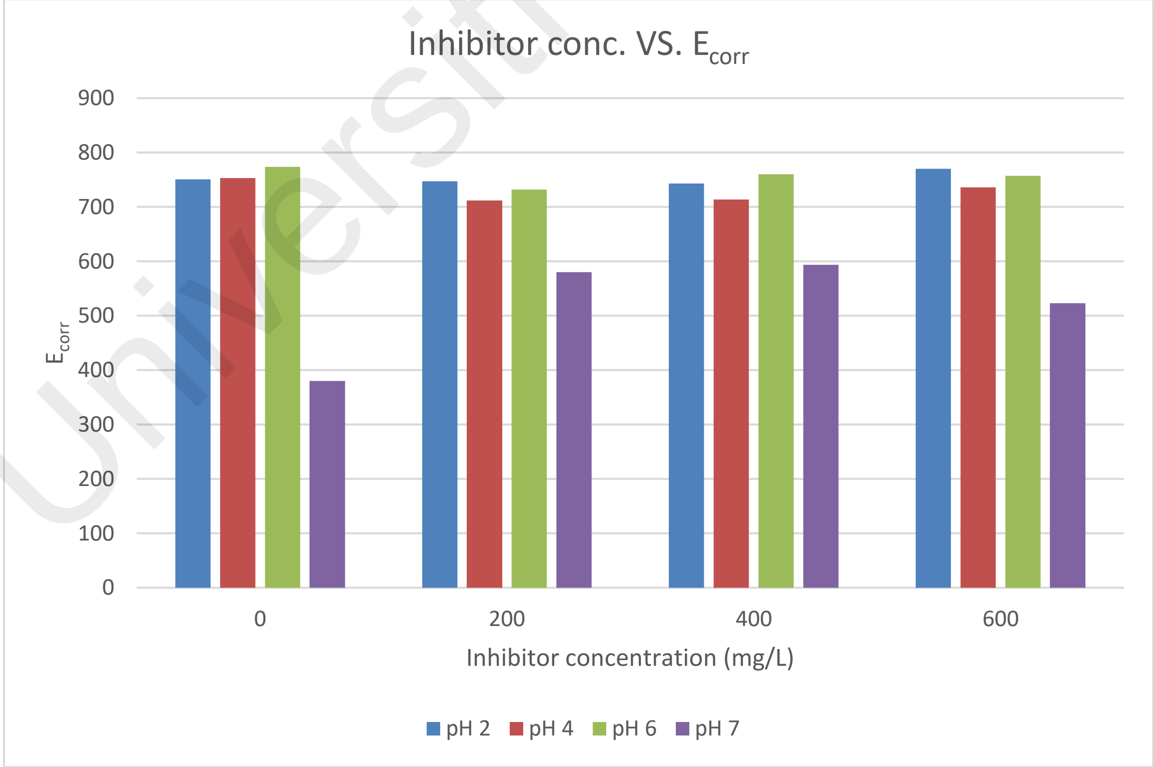

Figure 4.6: Corrosion potential against concentration of sodium sulphate inhibitor on aluminium alloy in different pH environments.

A trend of decrease in I_{corr} value when sodium sulphate is added in the acidic electrolytes until it reaches 400 mg/L, and then I_{corr} increases at 600 mg/L. The minimum corrosion density is found at 400 mg/L in pH 6 and the maximum corrosion density is at 600 mg/L in pH 6 as well. The effect of SO_4^{2-} concentration is prominent in pH 6 and 7, while barren in pH 4 and 7. The trend of chart for I_{corr} in pH 7 is almost stagnant and significantly low (almost zero) compared to corrosion density in acidic environments which means corrosion on aluminium does not affect by the presence of SO_4^{2-}.

According to the data in table 4.1, the values of β_c in blank acidic environments decreases with increasing pH. This is because as the pH of electrolyte increases, the concentration of H^+ decreases, resulting less cathodic reaction, while the β_a values in blank acidic environments are reasonably similar. comparatively higher than the β_a values in both uninhibited and inhibited samples. Based on table 4.1, the examined inhibitors shows a primarily cathodic nature in acidic environments, with β_c are generally larger than β_a in contrary to neutral environment which β_a are greater than β_c. Sodium sulphate incites corrosion on aluminium in neutral electrolyte via anodic reaction. As the pH increases, the dissolution of Al^{3+} also decreases (as mentioned in subs 2.1.4) because the anions Cl^- and SO_4^{2-} are responsible in donating electrons instead of aluminium alloy. It can be deduced that SO_4^{2-} could be an anodic-dominant inhibitor in acidic environments in consistent with the result presented by Abdallah et al. (2019) and Chen et al. (2021), where the organic inhibitors act as anodic-dominant in HCl solution. Whilst SO_4^{2-} cathodic-dominant inhibitor in neutral environment due to increases reaction in cathodic area because hydrogen receiving many electrons from the inhibitor.

From the graph in figure 4.6, E_{corr} in acidic electrolytes have trivial change with increasing inhibitor concentration and the values accumulated between -710 mV to -780 mV. The maximum difference of E_{corr} is 42 mV which in pH 4 electrolyte.

In neutral electrolyte, E_{corr} is higher in the presence of sodium sulphate compared to the absence of sodium sulphate, hardly exceeding any E_{corr} values in acidic environments.

4.1.3 Corrosion rates and inhibition efficiency

Table 4.2: The rate of corrosion and IE% of aluminium in various environments at ambient temperature.

Environment	Conc. of inhibitor (mg/L)	Corrosion rates (mils/y)	Corrosion reduction (mils/y)	IE (%)
pH 2	Blank	2.139	-	-
	200	1.712	0.428	19.72
	400	1.132	1.007	46.79
	600	1.327	0.813	38.58
pH 4	Blank	2.224	-	-
	200	1.065	1.159	51.51
	400	0.739	1.485	67.38
	600	1.723	0.501	23.94
pH 6	Blank	1.239	-	-
	200	0.901	0.339	20.45
	400	0.659	0.580	22.42
	600	1.003	0.237	18.22
pH 7	Blank	0.014	-	-
	200	0.047	-0.042	-61.84
	400	0.056	-0.042	-83.35
	600	0.047	-0.033	-45.99

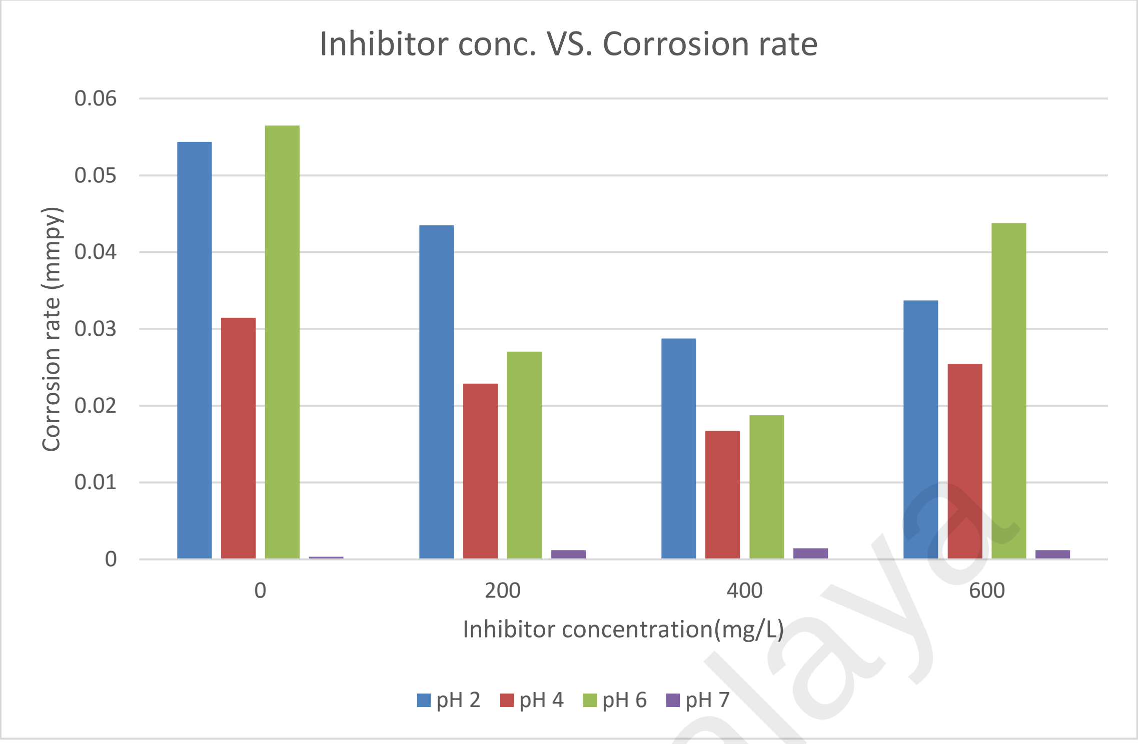

Figure 4.7: The graph of concentration of inhibitor against corrosion rate in acidic environments.

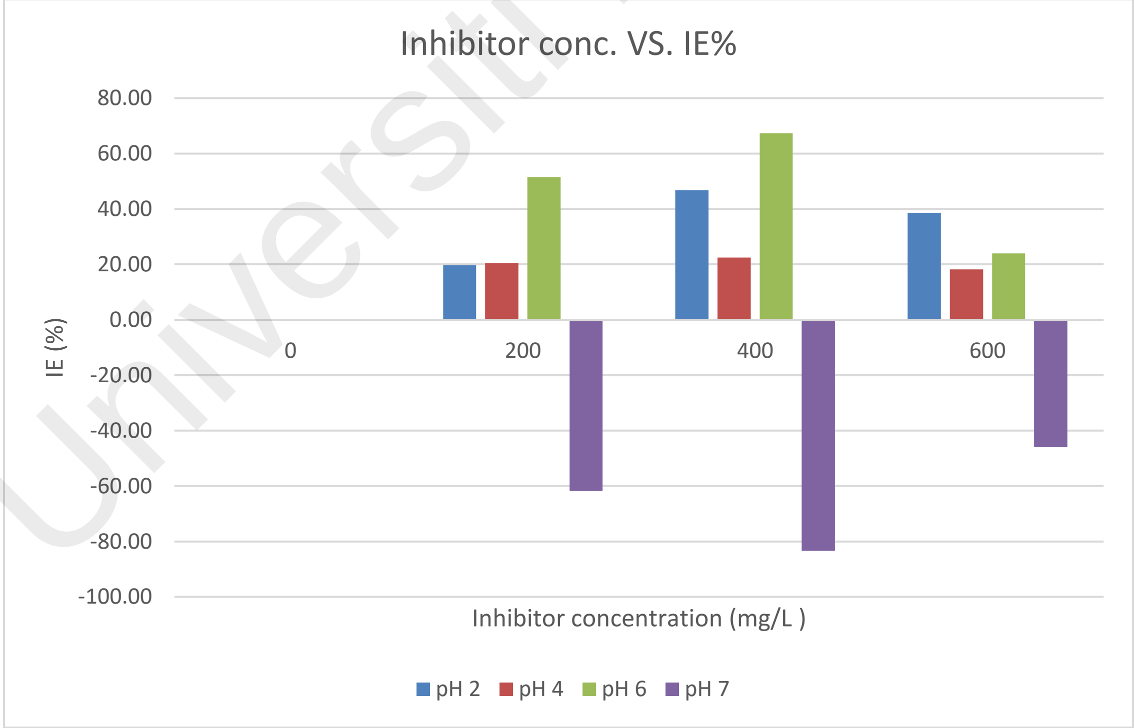

Figure 4.8: The graph of concentration of inhibitor against inhibition efficiency in acidic environments.

Based on the calculated corrosion rates in table 4.2, the aluminium corrodes faster in acidic environments than the average corrosion of aluminium in atmosphere because of the Cl^- (Ahmad, 2006). Cl^- in hydrochloric acid is easily adsorbed to the metal surface and weaken the protective film, in result exposing more surface of metal for corrosion (Chen et al., 2022).The maximum corrosion reduction is 1.007 mils/y in pH 2, 1.485 mils/y in pH 4, and 0.580 mils/y in pH 6 which all occurred at 400 mg/L sodium sulphate concentration whereas the minimum reduction happened at 600 mg/L concentration in pH 6 electrolyte with rate of 0.237 mils/y, which is quite remarkable in the presence of sodium sulphate even though the efficiency only at 18.22%. This proves that the concentration of SO_4^{2-}-containing inhibitor plays a critical role in supressing corrosion. At ambient temperature, sodium sulphate reaches 67.38% efficiency in inhibiting corrosion on aluminium. In general, table 4.2 shows the corrosion rates are sufficiently high for pitting to take place on aluminium samples in acidic environments though pitting in not expected to occur in the positive hysteresis shown in the polarisation curves discussed in subchapter 4.1.1. Therefore, it could be either Cl^- or SO_4^{2-}, or both anions are responsible for the pitting on aluminium in acidic environment with the presence of sulphate inhibitor.

The corrosion rate of aluminium in neutral solution increases sparsely with increasing sodium sulphate concentration. Although the presence of sodium sulphate give rise to corrosion rate, but not notably in long period of time. It can be concluded that SO_4^{2-} gives insignificant effect for corrosion to happen in this environment. The compound that responsible for corrosion to happen in neutral environment is O_2 and H^+ by donating lone pairs of electrons on metal surface and receiving electrons.

Discussion kena tambah mechanism of substrate dengan solution.

4.2 Weight loss measurement for acidic environments

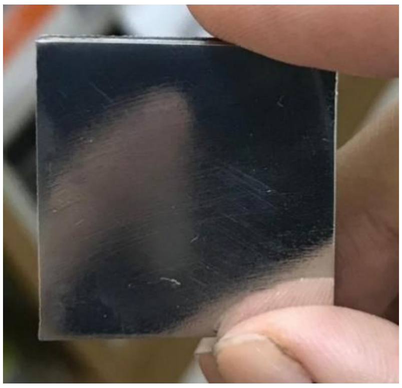

Figure 4.9: The polished 5052 aluminium alloy specimen before immersion.

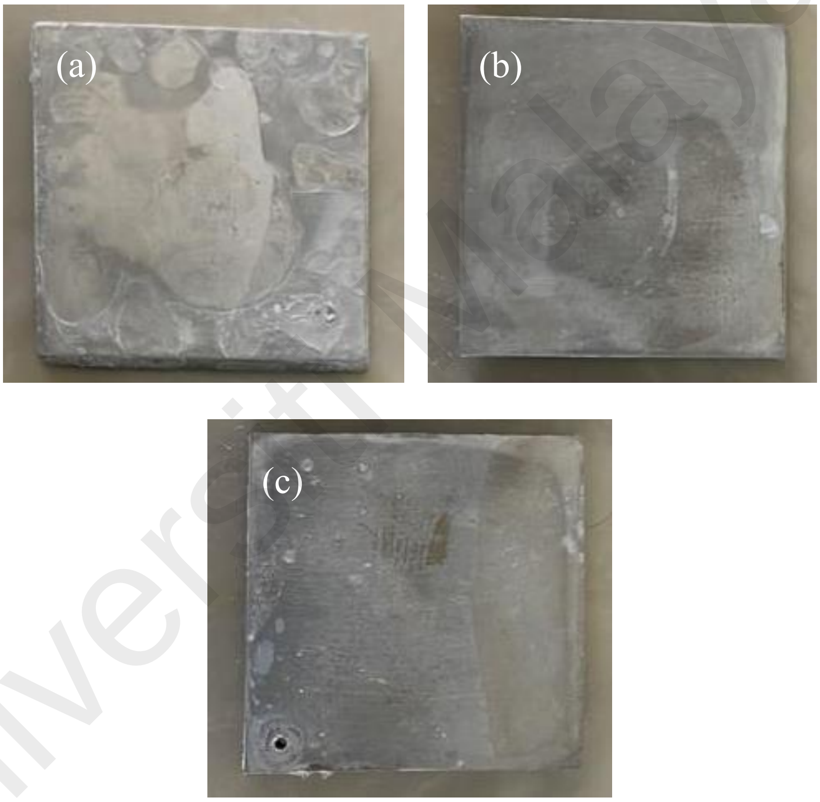

Figure 4.10: Photographs of 5052 aluminium alloy specimens in (a) pH 2, (b) pH 4 and (c) pH 6 subsequent to immersion for 7 days at room temperature.

From figure 4.10, the aluminium samples are deteriorated heavily after immersion in acidic electrolytes in ambient conditions after seven days.

Table 4.3: Parameters of weight loss tests for aluminium alloy in acidic environment.

	pH 2	**pH 4**	**pH 6**
Weight before immersion (g)	5.5130	5.6786	5.5651
Weight after immersion (g)	5.5108	5.6769	5.5638
Weight loss (g)	0.0022	0.0017	0.0013
Weight loss, ΔW (mg)	2.2000	1.7000	1.3000
Corrosion rates (mmpy)	0.0511	0.0395	0.0302
Corrosion rates (mils/y)	2.0130	1.5550	1.1890

According to table 4.3, the calculated corrosion rate of aluminium is higher than corrosion rates from the Tafel plots extrapolation, but the trend is consistent. It is found that the aluminium corrodes faster in pH 2, followed by pH 4 and pH 6. It is safe to deduce that the chemistry of the pH alone affected the corrosion behaviour of aluminium and promptly affecting the inhibiting properties of the corrosion inhibitor. Weight loss method was employed to support the result of corrosion from acidic environment on aluminium alloy specimens.

4.3 Optical microscopy images study

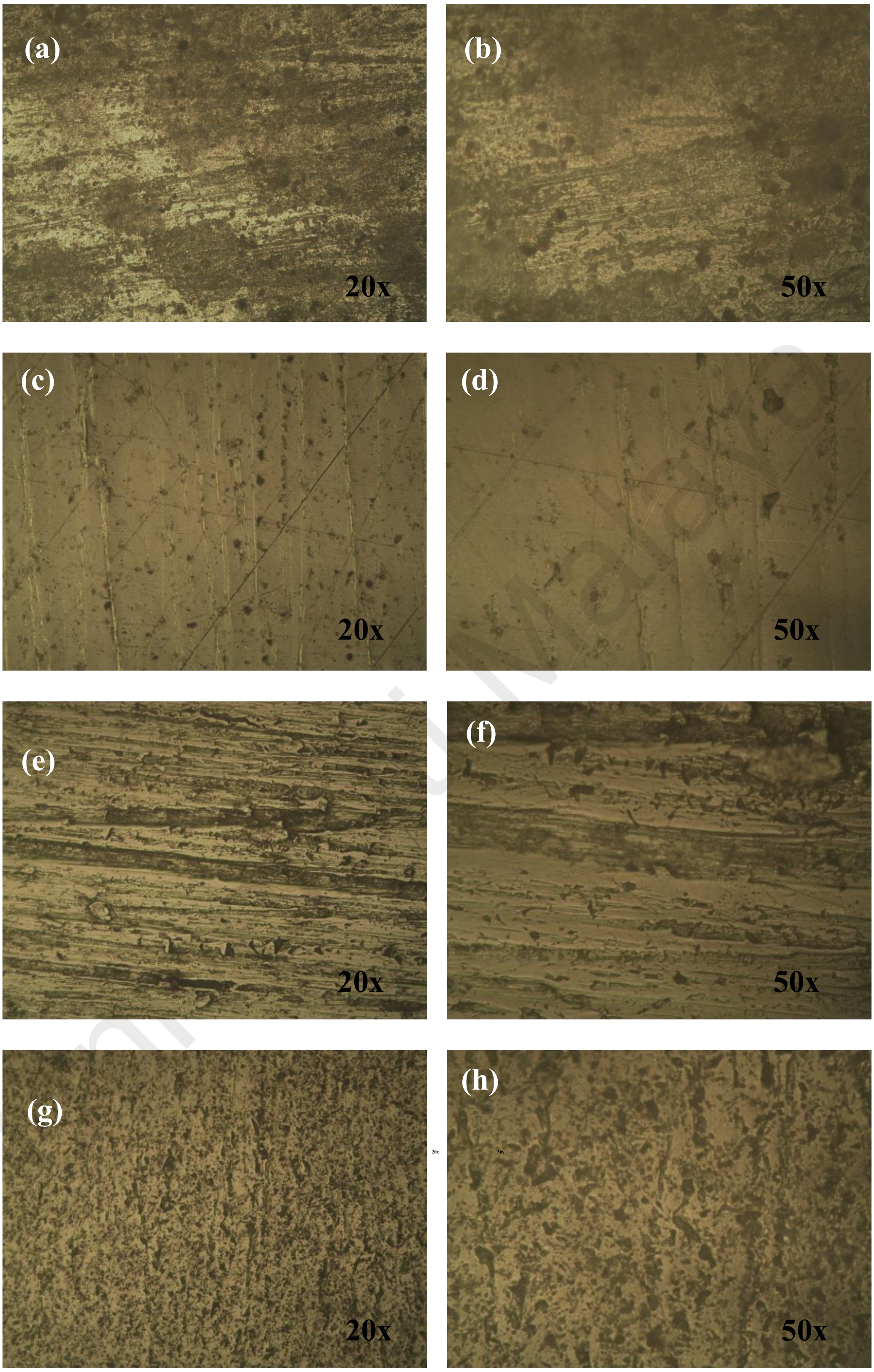

Figure 4.11: Optical microscopy images of 5052 aluminium alloy specimen at (a)(b) without inhibitor, (c)(d) 200 mg/L, (e)(f) 400 mg/L, and (g)(h) 600 mg/L concentration in pH 2.

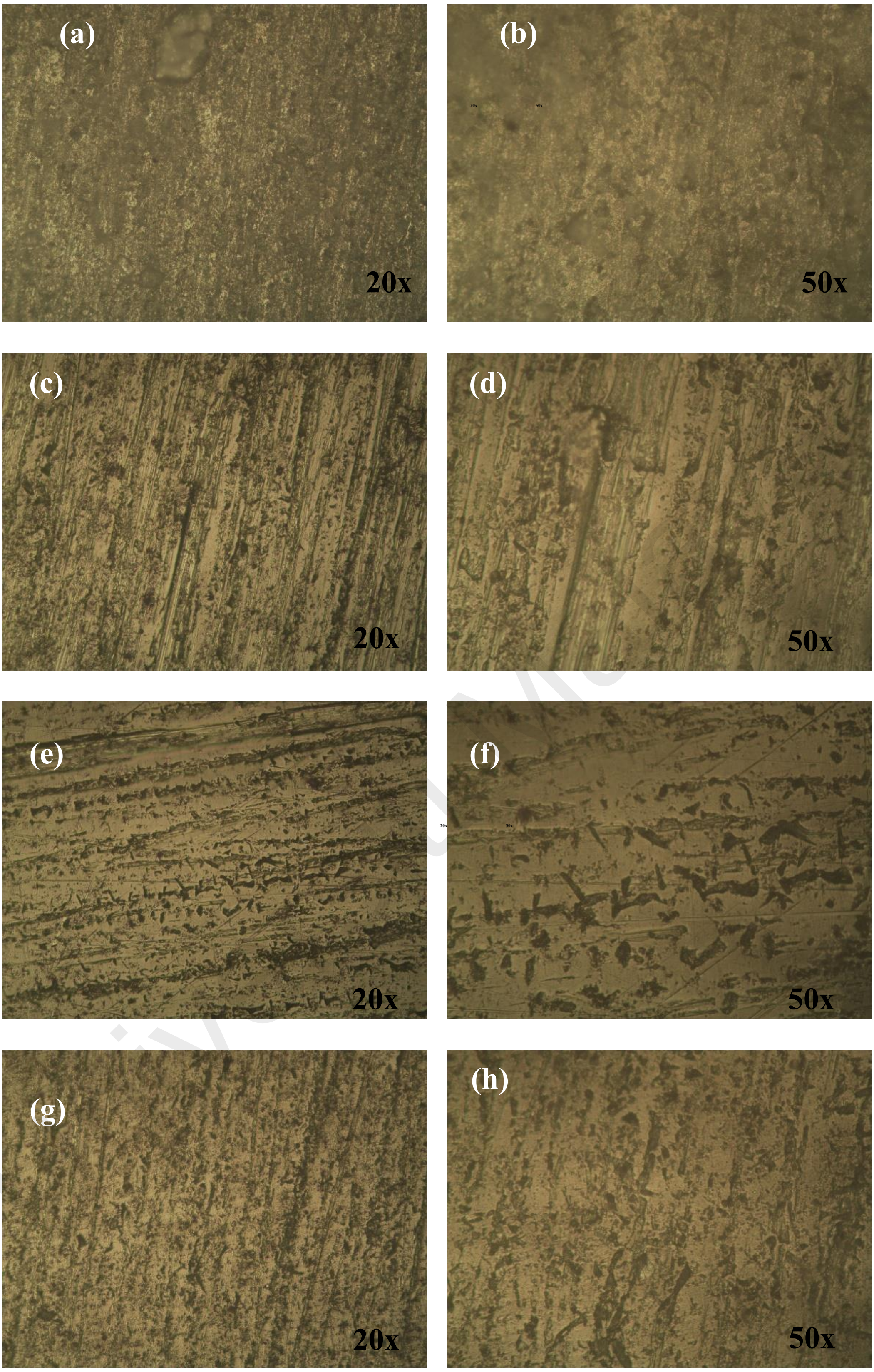

Figure 4.12: Optical microscopy images of 5052 aluminium alloy specimen at (a)(b) without inhibitor, (c)(d) 200 mg/L, (e)(f) 400 mg/L, and (g)(h) 600 mg/L concentration in pH 4.

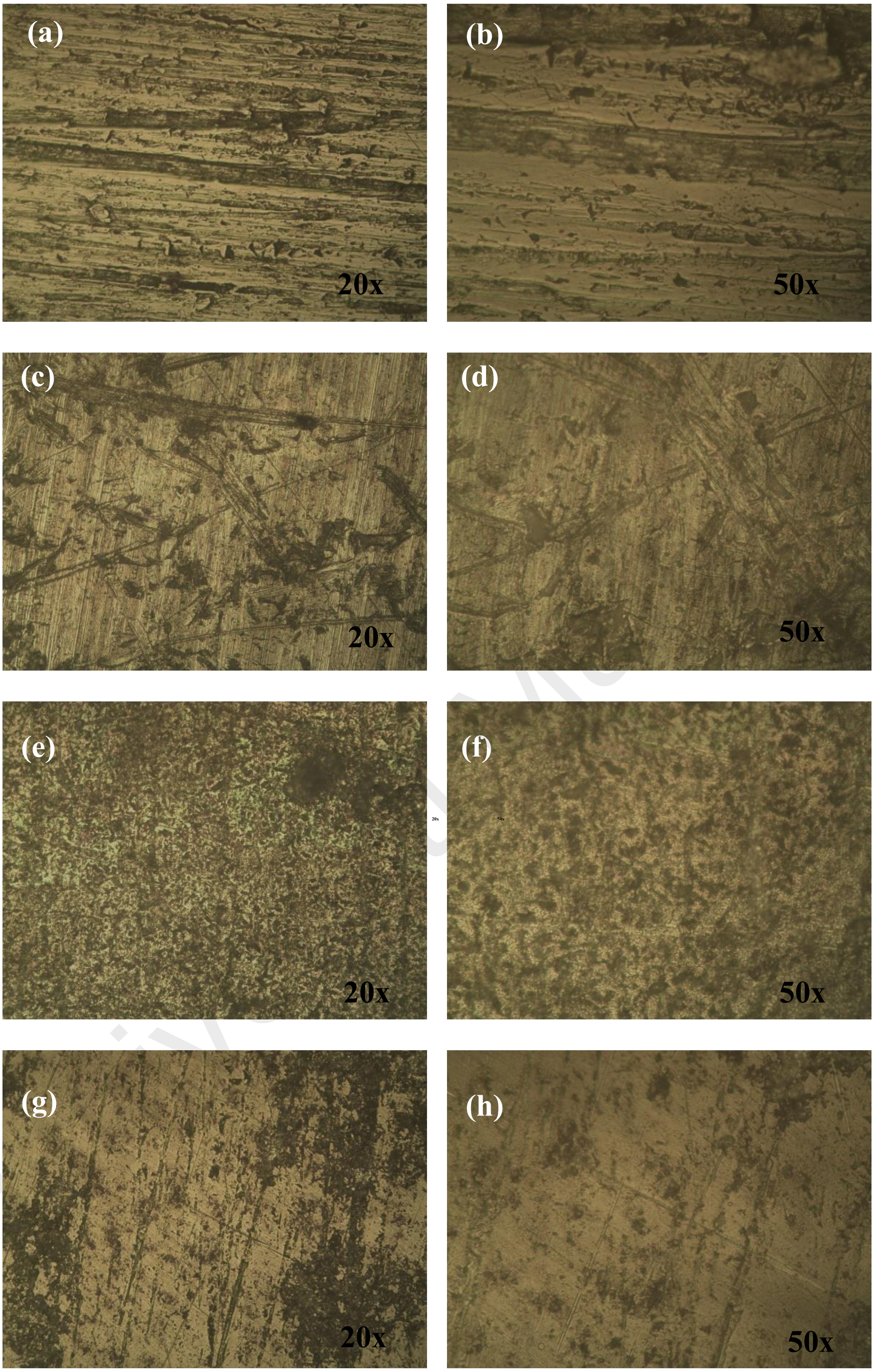

Figure 4.13: Optical microscopy images of 5052 aluminium alloy specimen at (a)(b) without inhibitor, (c)(d) 200 mg/L, (e)(f) 400 mg/L, and (g)(h) 600 mg/L concentration in pH 6.

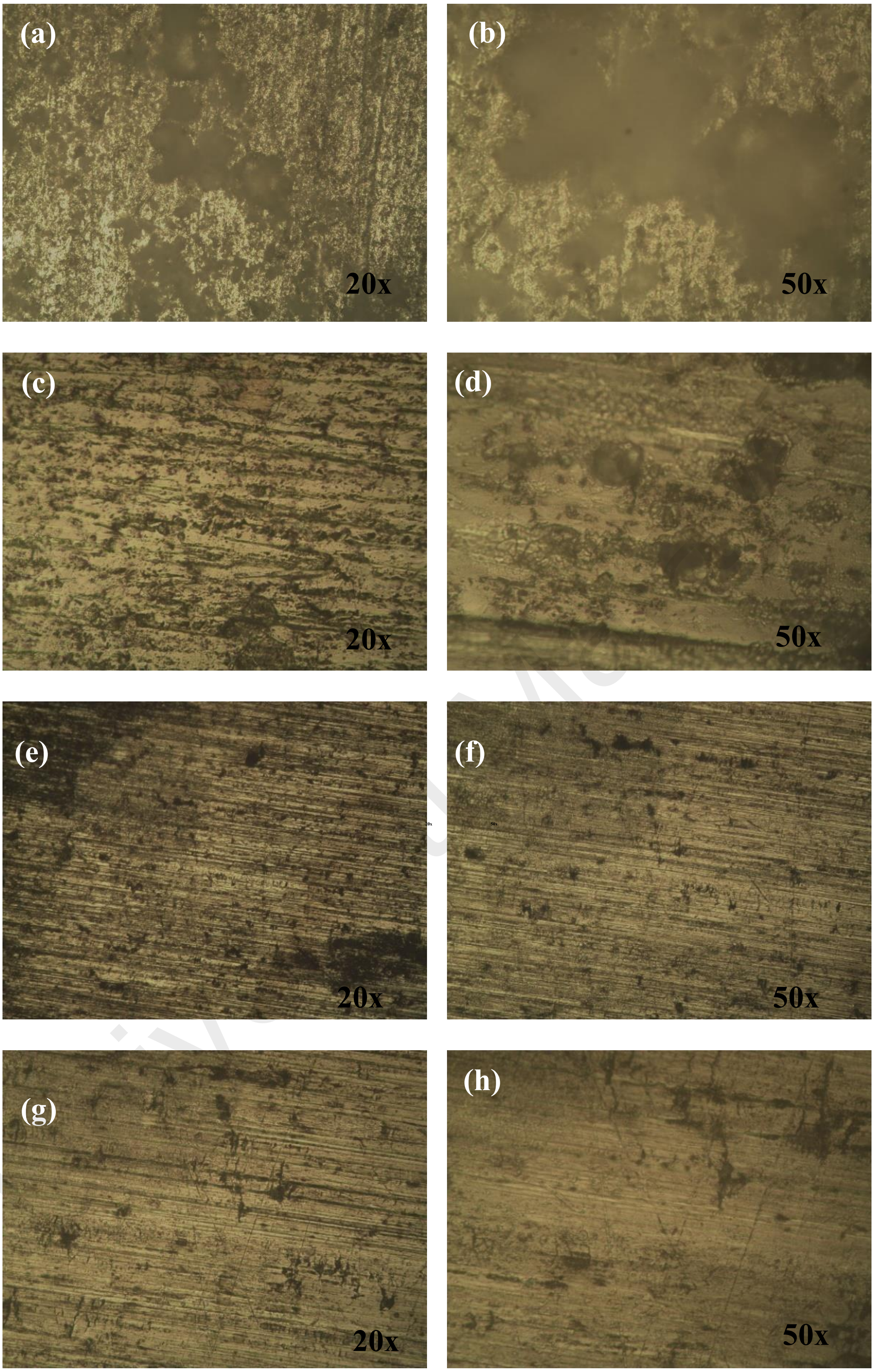

Figure 4.14: Optical microscopy images of 5052 aluminium alloy specimen at (a)(b) without inhibitor, (c)(d) 200 mg/L, (e)(f) 400 mg/L, and (g)(h) 600 mg/L concentration in pH 7.

Based on figure 4.11 – 4.14, are showing images with 20x and 50x magnification of aluminium samples. The images for 5x and 10x magnifications do not provide enough information of the surface (Appendix B). The morphological images of aluminium sample without sodium sulphate are extensively corroded with majority of pitting (figure 4.11, 4.12 and 4.13 (a)(b)). These conditions imply that hydrochloric acid is corroding aluminium alloy vigorously. Hydrochloric acid is an exception from other aggressive environment where most of the corrosion precipitates may be dissolved in the electrolyte because of the presence of chloride ion. Chloride is a small-sized anion that can easily adsorbed on the metal surface and breaks the protective layer on the surface of aluminium alloy, resulting a high corrosion rate. The holes and cavities on aluminium surface in pH 2 is more obvious and articulated under 50x magnification, and not prominent in pH 4 and pH 6 possibly due to high Cl^- and H^+ concentrations in lower pH electrolyte. As the pH decreases from 6 to 2, the concentration of Cl^- and H^+ increases. High concentration of H+ also promotes corrosion via cathodic reaction which is consistent with the decreasing value of β_c value from pH 2, followed by pH 4 and lastly pH 6 (table 3). The little increment of β_a value with increasing pH of electrolyte gives negligible general corrosion on the metal surface.

Based on Figure 4.11, some localised effects of corrosion are seen with some general corrosion on the surface of the sample in acidic solutions with inhibitor due to the action of Cl^- in hydrochloric acid and SO_4^{2-} from sodium sulphate . At 200 mg/L, majority of the surface area seems not to be affected by corrosion, corrosion cavities are plainly apparent. because of localised corrosion reactions of Cl^- on the metal surface. The cavities appeared more rapidly as the concentration increases as a consequence of Cl^- and SO_4^{2-} disrupting the protective barrier, forming in a pitted surface at regions on the metal, predominantly in zones with defects. Pit formation is basically due to adsorption and chemical interaction of Cl^- at these flaws in the surface oxide film.

Mild degradation of aluminium alloy morphology occurred in pH 2 and pH 4 solution after sodium sulphate is added due to the action of SO_4^{2-}. It is discussed by Chen et al. (2022) that SO_4^{2-} have stronger adsorption compared to Cl^- in the passive film on metal surface. SO_4^{2-} has bigger molecular size than Cl^-, provide stronger bond in the protective film, thus lessen the metal dissolution and H^+ attack. Observation on the morphological images of aluminium samples in pH 7 confirms the scarce formation of pitting on metal surface. The pitting and holes formed are very few compared to the samples in acidic environments. This is because of the absence of Cl^- in the electrolyte that usually induced pitting in acidic solutions. According to Loto and Babalola (2019), the presence of SO_4^{2-} without Cl^- could weaken the bonds on metal surface and causing the release of metal ions into the electrolytes which favours corrosion to happen. Hence, the big cavities that appeared on the aluminium surfaces in neutral electrolyte is due to the presence of SO_4^{2-}. It infers that SO_4^{2-} has the potential to cause localised corrosion or pitting, induced fracture along cavities in the protective oxide barrier which subjected to occur at random sites on the surface instead of blocking it from happening. The present work is not enough to confirm the inhibition mechanism of SO_4^{2-} on aluminium surfaces and how it causes pitting corrosion. Some adsorption measurements would be needed to confirm the nature of SO_4^{2-} in acidic and neutral environments on aluminium surface. The significant of SO_4^{2-} concentration to inhibit corrosion has not been fully examined. Optical microscope analysis is not enough to study the pitting corrosion so microanalytical analysis would be needed to determine the pitting morphology. From the overall specimens, there is no white precipitates formed on the aluminium alloy surfaces which means SO_4^{2-} is not a precipitate-typed inhibitor in both acidic and neutral environments. Passivation also does not occur significantly as the potentiodynamic polarization results show that there is a slight effect on the reduction sites in cathodic area of aluminium, which reported that SO_4^2 behaves like the other organic inhibitors (subchapter 2.2.5).

CHAPTER 5: CONCLUSION

The chloride attack is the main reason for the corrosion of the aluminium alloy to happen in acidic solutions. The combined action of chloride and sulphate seems to be able to suppress corrosion on aluminium alloy in the acidic solutions. Despite the relatively small size, the nature of Cl^- have significant impact on the deterioration of surface properties of metal alloys in acidic environment especially at pH 2 was quite minimal based on the optical morphology images. The potentiodynamic polarisation can reveal the corrosion mechanism of 5052 aluminium alloy which is anodic-dominant in acidic and cathodic-dominant in neutral environment. The optimum concentration of SO_4^{2-} is important to achieve maximum corrosion reduction. At ambient temperature, SO_4^{2-} has accomplished the highest inhibition efficiency with corrosion rate 0.739 mils/y on 5052 aluminium alloy in pH 4 at 400 mg/L concentration. The corrosion efficiency reduces as concentration is higher than 600 mg/L because sodium sulphate has reached its utmost adsorption on metal surface.

It is visible passivation behaviour when sodium sulphate inhibitor is added into the acidic electrolyte, which confirms the presence of SO_4^{2-} leading to breakdown of the passive film after sufficient displacement of Cl^- at the transpassive region. The inhibition effects of sodium sulphate on the samples increases with increasing its concentration and reaches a limiting value. The limiting value is related to the complete formation of monolayer film on the adsorbate over the surface of metal which in this research project, the limiting value is at 400 mg/L^{-1} at acidic environments. When the Cl^- and SO_4^{2-} are presence in a mixture together, sulphate ions will dominate the reaction with metal surface which reduces the ability of chloride ions to form pitting on metal surface. From the morphological images, the major corrosion reaction reactions that taking place in acidic environments is general and uniform.

Although SO_4^{2-} can introduce corrosion on metal surface, it is found that the corrosion rates are very slow and negligible. It can be concluded that the concentration of SO_4^{2-} used in this experiment was too high. The excess SO_4^{2-} penetrates the protective barrier and encourage corrosion than supressing it, therefore when 600 mg/L concentration into the electrolyte, the corrosion rate increases.

In neutral pH without the presence of Cl^-, it is highly plausible that the electron lone pairs of sulphate in the SO_4^{2-} paired with vacant orbital of aluminium and adsorbed on the aluminium alloy surface in the form of chemical bonds to provide larger coverage for corrosion to happen. Sodium sulphate stimulate corrosion as high as 83.4% from the original corrosion rate but in slow manner. SO_4^{2-} has negligible effect on aluminium alloy in neutral environment compared to the acidic environments in the long term although it might introduce pitting. The overall trend of the data offered the sign of an improved performance of corrosion behaviour by adding inhibitor into the acidic solutions at optimum concentration. The sodium sulphate reaches its maximum efficiency of 67.38% in pH 6 at 298K. The optical morphology images of the corrosion only depicted a vague observation on metal surface. The present work needs more work to do in the future such as using different x-ray instrument to study the micro images of the aluminium alloy surfaces such as SEM. To enhance the inhibition efficiency, the environment temperature could be altered and use instrument such as EDX to investigate the type of compounds that appear on metal surface and study the sodium sulphate adsorption behaviour with Langmuir adsorption isotherm to confirm the SO_4^{2-} activity on aluminium surface.

REFERENCES

Abdallah, M., Gad, E. A. M., Sobhi, M., Al-Fahemi, J. H., & Alfakeer, M. M. (2019). Performance of tramadol drug as a safe inhibitor for aluminum corrosion in 1.0 M HCl solution and understanding mechanism of inhibition using DFT. *Egyptian Journal of Petroleum*, *28*(2), 173-181. https://doi.org/https://doi.org/10.1016/j.ejpe.2019.02.003

Ahmad, Z. (2006). CHAPTER 10 - ATMOSPHERIC CORROSION. In Z. Ahmad (Ed.), *Principles of Corrosion Engineering and Corrosion Control* (pp. 550-575). Butterworth-Heinemann. https://doi.org/https://doi.org/10.1016/B978-075065924-6/50011-8

Bai, B., Xiao, G., Deng, L., Zhang, N., Chen, C., Bu, Y., & Che, D. (2021). A study on corrosion behavior of 15CrMo in saturated saline steam with sodium sulfate. *Corrosion Science*, *181*, 109240. https://doi.org/https://doi.org/10.1016/j.corsci.2021.109240

Basik, M., & Mobin, M. (2020). Chondroitin sulfate as potent green corrosion inhibitor for mild steel in 1 M HCl. *Journal of Molecular Structure*, *1214*, 128231. https://doi.org/https://doi.org/10.1016/j.molstruc.2020.128231

Beccaria, A. M., & Poggi, G. (1987). Aluminum Corrosion in Slightly Alkaline Sodium Sulfate Solutions at Different Hydrostatic Pressures. *Corrosion*, *43*(3), 153-158. https://doi.org/10.5006/1.3583128

Cen, H., Zhang, X., Zhao, L., Chen, Z., & Guo, X. (2019). Carbon dots as effective corrosion inhibitor for 5052 aluminium alloy in 0.1 M HCl solution. *Corrosion Science*, *161*, 108197. https://doi.org/https://doi.org/10.1016/j.corsci.2019.108197

Chen, T., Gan, H., Chen, Z., Chen, M., & Fu, C. (2021). Eco-friendly approach to corrosion inhibition of AA5083 aluminum alloy in HCl solution by the expired Vitamin B1 drugs. *Journal of Molecular Structure*, *1244*, 130881. https://doi.org/https://doi.org/10.1016/j.molstruc.2021.130881

Chen, Z., Wei, Z., Chen, Y., Nong, Y., & Yi, C. (2022). Molecular insight into iron corrosion induced by chloride and sulphate. *Computational Materials Science*, *209*, 111429. https://doi.org/https://doi.org/10.1016/j.commatsci.2022.111429

Coulson, C. A. (1969). d Electrons and Molecular Bonding. *Nature*, *221*(5186), 1106-1110. https://doi.org/10.1038/2211106a0

Cui, L., Hang, M., Huang, H., & Gao, X. (2021). Experimental study on multi-component corrosion inhibitor for steel bar in chloride environment. *Construction and Building Materials*, *313*, 125533. https://doi.org/https://doi.org/10.1016/j.conbuildmat.2021.125533

Ćurković, L., Jelača, M. F., & Kurajica, S. (2008). Corrosion behavior of alumina ceramics in aqueous HCl and H2SO4 solutions. *Corrosion Science*, *50*(3), 872-878. https://doi.org/https://doi.org/10.1016/j.corsci.2007.10.008

dissimilar (metal) corrosion. (2014). In H. Herrmann & H. Bucksch (Eds.), *Dictionary Geotechnical Engineering/Wörterbuch GeoTechnik: English-German/Englisch-Deutsch* (pp. 393-393). Springer Berlin Heidelberg. https://doi.org/10.1007/978-3-642-41714-6_42644

El-Lateef, H. M. A., El-Sayed, A.-R., Mohran, H. S., & Shilkamy, H. A. S. (2019). Corrosion inhibition and adsorption behavior of phytic acid on Pb and Pb–In alloy surfaces in acidic chloride solution. *International Journal of Industrial Chemistry*, *10*(1), 31-47. https://doi.org/10.1007/s40090-019-0169-4

Farfan-Cabrera, L. I., Rodríguez-Bravo, G. A., Godínez-Salcedo, J. G., Resendiz-Calderon, C. D., Salgado-Sviercovich, J. S., & Moreno-Ríos, M. (2021). A crevice corrosion assessment method for joints of mechanical components sealed with composite structure gaskets – The case of the engine cylinder head/mono-block joint. *Engineering Failure Analysis*, *119*, 104981. https://doi.org/https://doi.org/10.1016/j.engfailanal.2020.104981

Hassan, R. M., Ibrahim, S. M., Takagi, H. D., & Sayed, S. A. (2018). Kinetics of corrosion inhibition of aluminum in acidic media by water-soluble natural polymeric chondroitin-4-sulfate as anionic polyelectrolyte inhibitor. *Carbohydrate Polymers*, *192*, 356-363. https://doi.org/https://doi.org/10.1016/j.carbpol.2018.03.066

Homborg, A. M., Olgiati, M., Denissen, P. J., & Garcia, S. J. (2022). An integral non-intrusive electrochemical and in-situ optical technique for the study of the effectiveness of corrosion inhibition. *Electrochimica Acta*, *403*, 139619. https://doi.org/https://doi.org/10.1016/j.electacta.2021.139619

Hussey, B., & Wilson, J. (1998). Alloy Data. In B. Hussey & J. Wilson (Eds.), *Light Alloys: Directory and Databook* (pp. 141-349). Springer US. https://doi.org/10.1007/978-1-4615-5777-7_3

Ishwara Bhat, J., & Alva, V. D. P. (2011). A Study of Aluminium Corrosion Inhibition in Acid Medium by an Antiemitic Drug. *Transactions of the Indian Institute of Metals*, *64*(4), 377-384. https://doi.org/10.1007/s12666-011-0102-9

Ismail, I., Harun, M. K., & Yahya, M. Z. A. (2019). Corrosion protection of mild steel by the synergetic effect of sodium dodecylbenzenesulfonates and zinc sulfate in sodium chloride solution. *Int J Electrochem Sci*, *14*, 11491-11508.

Jessima, S. J. H. M., Berisha, A., Srikandan, S. S., & S, S. (2020). Preparation, characterization, and evaluation of corrosion inhibition efficiency of sodium lauryl sulfate modified chitosan for mild steel in the acid pickling process. *Journal of Molecular Liquids*, *320*, 114382. https://doi.org/https://doi.org/10.1016/j.molliq.2020.114382

Ju, H., Liu, S., Zhang, W., Yang, Y., & Duan, J. (2021). Investigation of pitting corrosion and hydrogen evolution of aluminum and AA2024 alloy by simultaneous electrochemical measurements and imaging. *Electrochemistry Communications*, *132*, 107135. https://doi.org/https://doi.org/10.1016/j.elecom.2021.107135

Kamble, P. A., Deshpande, P. P., & Vagge, S. T. (2022). Numerical investigation of galvanic corrosion between galvanized steel and mild steel in bolted joint. *Materials Today: Proceedings*, *50*, 1923-1929. https://doi.org/https://doi.org/10.1016/j.matpr.2021.09.316

Kaufman, J., Racek, J., Cieslar, M., Minárik, P., Steiner, M. A., Mannava, S. R., Vasudevan, V. K., Sharma, A., Böhm, M., Brajer, J., Pilař, J., Pína, L., & Mocek, T. (2022). The effect of laser shock peening with and without protective coating on intergranular corrosion of sensitized AA5083. *Corrosion Science*, *194*, 109925. https://doi.org/https://doi.org/10.1016/j.corsci.2021.109925

Kenney, J. A., & Hwang, G. S. (2009). MATERIALS | Etching. In J. Garche (Ed.), *Encyclopedia of Electrochemical Power Sources* (pp. 625-631). Elsevier. https://doi.org/https://doi.org/10.1016/B978-044452745-5.00082-4

Koundal, M., Singh, A. K., & Sharma, C. (2022). Study on the effect of imidazolium ionic liquid as a modulator of corrosion inhibition of anionic surfactant sodium dodecyl sulfate (SDS) on mild steel in sodium chloride solution. *Journal of Molecular Liquids*, 118561.

L'Haridon-Quaireau, S., Laot, M., Colas, K., Kapusta, B., Delpech, S., & Gosset, D. (2020). Effects of temperature and pH on uniform and pitting corrosion of aluminium alloy 6061-T6 and characterisation of the hydroxide layers. *Journal of Alloys and Compounds*, *833*, 155146. https://doi.org/https://doi.org/10.1016/j.jallcom.2020.155146

Li, S., & Church, B. C. (2018). Effects of sulfate and nitrate anions on aluminum corrosion in slightly alkaline solution. *Applied Surface Science*, *440*, 861-872. https://doi.org/https://doi.org/10.1016/j.apsusc.2018.01.108

Li, Y., Lu, X., Mei, D., Zhang, T., & Wang, F. (2021). Passivation of corrosion product layer on AM50 Mg by corrosion inhibitor. *Journal of Magnesium and Alloys*. https://doi.org/https://doi.org/10.1016/j.jma.2021.11.020

Liang, M., Melchers, R., & Chaves, I. (2018). Corrosion and pitting of 6060 series aluminium after 2 years exposure in seawater splash, tidal and immersion zones. *Corrosion Science*, *140*, 286-296. https://doi.org/https://doi.org/10.1016/j.corsci.2018.05.036

Loto, R. T., & Babalola, P. (2019). Electrochemical analysis of SiC composite additions at 7.5% weight content on the corrosion resistance of monolithic aluminium alloy in sulphate–chloride solution. *Journal of Materials Research and Technology*, *8*(3), 2517-2527. https://doi.org/https://doi.org/10.1016/j.jmrt.2019.03.001

Maddela, S., & Carlson, B. E. (2019). Corrosion Characterization of Resistance Spot-Welded Aluminum and Steel Couple. *Journal of Manufacturing Science and Engineering*, *141*(11), 111010.

Metikoš-Huković, M., Babić, R., Grubač, Z., & Brinć, S. (1994). Impedance spectroscopic study of aluminium and Al-alloys in acid solution: inhibitory action of nitrogen containing compounds. *Journal of Applied Electrochemistry*, *24*(8), 772-778. https://doi.org/10.1007/BF00578093

Monticelli, C. (2018). Corrosion Inhibitors. In K. Wandelt (Ed.), *Encyclopedia of Interfacial Chemistry* (pp. 164-171). Elsevier. https://doi.org/https://doi.org/10.1016/B978-0-12-409547-2.13443-2

Na, K.-H., & Pyun, S.-I. (2007). Electrochemical noise analysis of corrosion of pure aluminium in alkaline solution in the presence of SO42− ion, NO3− ion and Na2S additives. *Electrochimica Acta*, *52*(13), 4363-4373. https://doi.org/https://doi.org/10.1016/j.electacta.2006.12.029

Nathiya, R. S., Perumal, S., Murugesan, V., Anbarasan, P. M., & Raj, V. (2017). Agarose as an Efficient Inhibitor for Aluminium Corrosion in Acidic Medium: An Experimental and Theoretical Study. *Journal of Bio- and Tribo-Corrosion*, *3*(4), 44. https://doi.org/10.1007/s40735-017-0103-2

Nnaji, N., Nwaji, N., Fomo, G., Mack, J., & Nyokong, T. (2019). Inhibition of Aluminium Corrosion Using Benzothiazole and Its Phthalocyanine Derivative. *Electrocatalysis*, *10*(4), 445-458. https://doi.org/10.1007/s12678-019-00538-1

Nwanonenyi, S. C., Obasi, H. C., & Eze, I. O. (2019). Hydroxypropyl Cellulose as an Efficient Corrosion Inhibitor for Aluminium in Acidic Environments: Experimental and Theoretical Approach. *Chemistry Africa*, *2*(3), 471-482. https://doi.org/10.1007/s42250-019-00062-1

Pan, B., Sun, H., Shang, S.-L., Wen, W., Banu, M., Simmer, J. C., Carlson, B. E., Chen, N., Liu, Z.-K., Zheng, Z., Wang, P., & Li, J. (2021). Corrosion behavior in aluminum/galvanized steel resistance spot welds and self-piercing riveting joints in salt spray environment. *Journal of Manufacturing Processes*, *70*, 608-620. https://doi.org/https://doi.org/10.1016/j.jmapro.2021.08.052

Pedeferri, P. (2018a). Pourbaix Diagrams. In P. Pedeferri (Ed.), *Corrosion Science and Engineering* (pp. 57-72). Springer International Publishing. https://doi.org/10.1007/978-3-319-97625-9_4

Pedeferri, P. (2018b). Uniform Corrosion in Acidic and Aerated Solutions. In P. Pedeferri (Ed.), *Corrosion Science and Engineering* (pp. 145-167). Springer International Publishing. https://doi.org/10.1007/978-3-319-97625-9_8

Peng, C., Liu, Y.-w., Guo, M.-x., Gu, T.-z., Wang, C., Wang, Z.-y., & Sun, C. (2022). Corrosion and pitting behavior of pure aluminum 1060 exposed to Nansha Islands tropical marine atmosphere. *Transactions of Nonferrous Metals Society of China*, *32*(2), 448-460. https://doi.org/https://doi.org/10.1016/S1003-6326(22)65806-0

Pourbaix, M. (1991). Thermodynamics and Corrosion. In M. G. S. Ferreira & C. A. Melendres (Eds.), *Electrochemical and Optical Techniques for the Study and Monitoring of Metallic Corrosion* (pp. 1-30). Springer Netherlands. https://doi.org/10.1007/978-94-011-3636-5_1

Prakashaiah, B. G., Shetty, A. N., & Amitharani, B. E. (2018). 2-(4-(Diethylamino)-2-hydroxybenzyledene) Hydrazinecarboamide as Corrosion Inhibitor on AA2024-T3 Aluminium Alloy in 0.5 M Hydrochloric Acid Solution. *Surface Engineering and Applied Electrochemistry*, *54*(3), 286-296. https://doi.org/10.3103/S1068375518030109 \

Pyun, S. I., & Lee, W. J. (2001). The effect of prior Cl− ion incorporation into native oxide film on pure aluminium in neutral chloride solution on pit initiation. *Corrosion Science*, *43*(2), 353-363. https://doi.org/https://doi.org/10.1016/S0010-938X(00)00077-9

Pyun, S. i., Moon, S. M., Ahn, S. H., & Kim, S. S. (1999). Effects of Cl−, NO− 3 and SO2− 4 ions on anodic dissolution of pure aluminum in alkaline solution. *Corrosion Science*, *41*(4), 653-667. https://doi.org/https://doi.org/10.1016/S0010-938X(98)00132-2

Qian, S., Zhang, T., Chen, Y., Xie, J., Chen, Y., Lin, T., & Li, H. (2022). Effect of ultrasonic impact treatment on microstructure and corrosion behavior of friction stir welding joints of 2219 aluminum alloy. *Journal of Materials Research and Technology*, *18*, 1631-1642. https://doi.org/https://doi.org/10.1016/j.jmrt.2022.03.068

Raviprabha, K., & Ramesh, S. B. (2019). 5-(3-Pryridyl)-4H-1,2,4-triazole-3-thiol as Potential Corrosion Inhibitor for AA6061 Aluminium Alloy in 0.1 M Hydrochloric Acid Solution. *Surface Engineering and Applied Electrochemistry*, *55*(6), 723-733. https://doi.org/10.3103/S1068375519060103

Rodič, P., Lekka, M., Andreatta, F., Milošev, I., & Fedrizzi, L. (2021). The synergistic effect of cerium acetate and sodium sulphate on corrosion inhibition of AA2024-T3 at various temperatures. *Electrochimica Acta*, *370*, 137664. https://doi.org/https://doi.org/10.1016/j.electacta.2020.137664

Rodič, P., Milošev, I., Lekka, M., Andreatta, F., & Fedrizzi, L. (2019). Study of the synergistic effect of cerium acetate and sodium sulphate on the corrosion inhibition of AA2024-T3. *Electrochimica Acta*, *308*, 337-349. https://doi.org/https://doi.org/10.1016/j.electacta.2019.04.042

Ross, R. B. (1992). Aluminium Al. In R. B. Ross (Ed.), *Metallic Materials Specification Handbook* (pp. 1-67). Springer US. https://doi.org/10.1007/978-1-4615-3482-2_1

Sabet Bokati, K., & Dehghanian, C. (2018). Adsorption behavior of 1H-benzotriazole corrosion inhibitor on aluminum alloy 1050, mild steel and copper in artificial seawater. *Journal of Environmental Chemical Engineering*, *6*(2), 1613-1624. https://doi.org/https://doi.org/10.1016/j.jece.2018.02.015

Schweitzer, P. A. (2010). *Fundamentals of Corrosion Mechanisms, Causes, and Preventative Methods* (T. F. Group, Ed.). CRC Press.

Singh, A., Ansari, K. R., & Quraishi, M. A. (2020). Chondroitin sulfate as a green corrosion inhibitor for zinc in 26% ammonium chloride solution: Electrochemical and surface morphological analysis. *Colloids and Surfaces A:*

Physicochemical and Engineering Aspects, *607*, 125465. https://doi.org/https://doi.org/10.1016/j.colsurfa.2020.125465

Song, H., Xu, Z., Benabou, L., Yin, Z., Guan, H., Yan, H., Chao, L., Hu, Z., & Wang, X. (2021). Sodium dodecyl sulfate (SDS) as an effective corrosion inhibitor for Mg-8Li-3Al alloy in aqueous NaCl: A combined experimental and theoretical investigation. *Journal of Magnesium and Alloys*. https://doi.org/https://doi.org/10.1016/j.jma.2021.07.006

Szklarska-Smialowska, Z. (1991). Methods for Studying Corrosion Inhibition. In M. G. S. Ferreira & C. A. Melendres (Eds.), *Electrochemical and Optical Techniques for the Study and Monitoring of Metallic Corrosion* (pp. 545-570). Springer Netherlands. https://doi.org/10.1007/978-94-011-3636-5_15

Trompette, J.-L., & Lahitte, J.-F. (2021). Effects of some ion-specific properties in the electrocoagulation process with aluminum electrodes. *Colloids and Surfaces A: Physicochemical and Engineering Aspects*, *629*, 127507. https://doi.org/https://doi.org/10.1016/j.colsurfa.2021.127507

Usman, B. J., Scenini, F., & Curioni, M. (2020). Exploring the use of an AC-DC-AC technique for the accelerated evaluation of anticorrosion performance of anodic films on aluminium alloys. *Progress in Organic Coatings*, *144*, 105648. https://doi.org/https://doi.org/10.1016/j.porgcoat.2020.105648

Vargel, C. (2004). Chapter E.6 - Inorganic Salts. In C. Vargel (Ed.), *Corrosion of Aluminium* (pp. 417-441). Elsevier. https://doi.org/https://doi.org/10.1016/B978-008044495-6/50031-8

Verma, C., Verma, D. K., Ebenso, E. E., & Quraishi, M. A. (2018). Sulfur and phosphorus heteroatom-containing compounds as corrosion inhibitors: An overview [https://doi.org/10.1002/hc.21437]. *Heteroatom Chemistry*, *29*(4), e21437. https://doi.org/https://doi.org/10.1002/hc.21437

Ye, W., Pan, Y., He, L., Chen, B., Liu, J., Gao, J., Wang, Y., & Yang, Y. (2021). Chapter 3 - Design with modeling techniques. In H. D. Goodfellow & Y. Wang (Eds.), *Industrial Ventilation Design Guidebook (Second Edition)* (pp. 109-183). Academic Press. https://doi.org/https://doi.org/10.1016/B978-0-12-816673-4.00008-0

Zhang, Q.-H., Li, X.-R., Liu, P., Meng, X.-Z., Wu, L.-K., Luo, Z.-Z., & Cao, F.-H. (2021). Quantitative study of the kinetics of hydrogen evolution reaction on aluminum surface and the influence of chloride ion. *International Journal of Hydrogen Energy*, *46*(80), 39665-39674. https://doi.org/https://doi.org/10.1016/j.ijhydene.2021.09.189

Zhao, W., Zhou, S., & Wu, Z. (2017, 2017//). Double-Layer Corrosion Protection of Aluminium Pigments Applied in Water-Based Silver Ink. Advanced Graphic Communications and Media Technologies, Singapore.